Journal Name: Smart Materials and Devices

Manuscript NO: SMD_202673

Manuscript Type: Review

Manuscript Title: Single-component dual-band electrochromic materials and devices for smart optical and thermal management

Manuscript Author: Lu Chen[1], Chao Han[1,2], Binbin Liu[1], Wei Wang[3], Mingxin Ma[1], Yuer He[1], Yiran Wang[1], Bing Ding[1], Shengliang Zhang[1,2,*], Xiaogang Zhang[1,2]

Institution:

[1]Jiangsu Key Laboratory of Electrochemical Energy Storage Technologies, College of Materials Science and Technology, Nanjing University of Aeronautics and Astronautics, Nanjing 210016, Jiangsu, China.

[2]Shenzhen Research Institute, Nanjing University of Aeronautics and Astronautics, Shenzhen 518110, Guangdong, China.

[3]HongYuan Waterproof Technology Group Co. Ltd, Weifang 262735, Shandong, China.

[*]**Correspondence to:**

Shengliang Zhang, Jiangsu Key Laboratory of Electrochemical Energy Storage Technologies, College of Materials Science and Technology, Nanjing University of Aeronautics and Astronautics, Nanjing 210016, Jiangsu, China; Shenzhen Research Institute, Nanjing University of Aeronautics and Astronautics, Shenzhen 518110, Guangdong, China. E-mail: zhangsl@nuaa.edu.cn

ARTICLE IN PRESS

Cite this article:

Chen Lu, Han C, Liu B, Wang W, Ma M, He Y, et al. Single-component dual-band electrochromic materials and devices for smart optical and thermal management. Smart Mater Devices. 2027;3(2):202673. https://doi.org/10.70401/smd.2026.0070

Received: September 18, 2026 **Accepted:** November 17, 2026 **Published:** November 18, 2026

Abstract

Dual-band electrochromic materials capable of independently regulating visible (VIS) light and near-infrared (NIR) offer a promising pathway toward advanced solar management and energy-efficient devices. Compared with conventional multicomponent systems, single-component dual-band electrochromic materials enable spectrally selective modulation within a single active layer, simplifying device architectures while facilitating multifunctional integration. This review summarizes recent advances in single-component dual-band electrochromic materials and devices, focusing on material design, modulation mechanisms, and emerging applications. Representative inorganic and organic systems are discussed, highlighting strategies including defect engineering, ion intercalation, structural and morphological regulation, and molecular design for constructing distinct redox processes and spectrally separated absorption channels. The underlying mechanisms responsible for asynchronous VIS/NIR modulation, including localized surface plasmon resonance, polaron absorption, and stepwise redox reactions, are systematically analyzed. Furthermore, recent progress in multifunctional devices for energy-efficient smart windows and electrochromic energy-storage systems is reviewed. Finally, key challenges associated with material stability, scalable fabrication, device integration, and long-term durability are discussed, together with future perspectives toward large-area, flexible, low-voltage, and intelligent electrochromic systems. This review provides insights into the rational design and practical development of high-performance single-component dual-band electrochromic materials for next-generation adaptive optical and energy devices.

Keywords: Electrochromic, dual-band electrochromic materials, smart windows, spectral-selective modulation, photothermal regulation

ARTICLE IN PRESS

1.Introduction

The dual challenges of the energy crisis and climate change have brought building energy conservation into sharp global focus[1-3].Statistics indicate that building operations account for more than 30% of total societal end-use energy consumption, while cooling and heating losses through windows contribute approximately 20-40% of total building energy use[4-7].Therefore, developing highly efficient energy-saving window technologies has become an important pathway toward achieving the "dual-carbon" goals[8]. Electrochromic smart windows can reversibly modulate the optical properties of materials, including transmittance, reflectance, and absorptance, under an applied electric field[9,10].Combining active regulation, low energy consumption, and excellent environmental adaptability, electrochromic smart windows are widely regarded as a key solution for next-generation energy-efficient building glazing[11,12].

Conventional electrochromic materials have primarily focused on modulating the visible-light spectrum[13, 14]. However, approximately 50% of solar radiation energy lies in the near-infrared (NIR) region; regulating only visible light while neglecting the NIR allows substantial thermal radiation to penetrate through windows, thereby compromising energy-saving performance[15,16]. An ideal smart windows should independently regulate transmittance in the visible and near-infrared (NIR) regions in response to ambient climatic conditions and user demands, enabling multiple operating modes, such as "bright-warm", "bright-cool", and "dark-cool", thereby preserving natural daylighting while effectively blocking solar heat gain or maximizing solar heating in winter to substantially reduce the energy consumption of lighting and HVAC systems[17,18].

To achieve dual-band modulation, researchers have successively developed two main technological pathways: dual-component composites and single-component materials[19,20]. Although dual-component systems, such as ITO nanocrystal/NbO_x composite films[21]aand WO_3/VO_2 stacked structures[22] have demonstrated excellent dual-band modulation capabilities, their complex fabrication processes-necessitating precise matching of the operating voltage windows for both components and strict

ARTICLE IN PRESS

assurance of film microstructural uniformity-significantly increase the complexity of device design and manufacturing. In contrast, single-component dual-band electrochromic materials achieve independent modulation of the visible and near-infrared spectra utilizing a single active layer, which substantially simplifies device architectures and fabrication processes while preserving excellent optical modulation ranges and rapid response kinetics, thus emerging as a prominent research focus in the field of electrochromics in recent years[23].

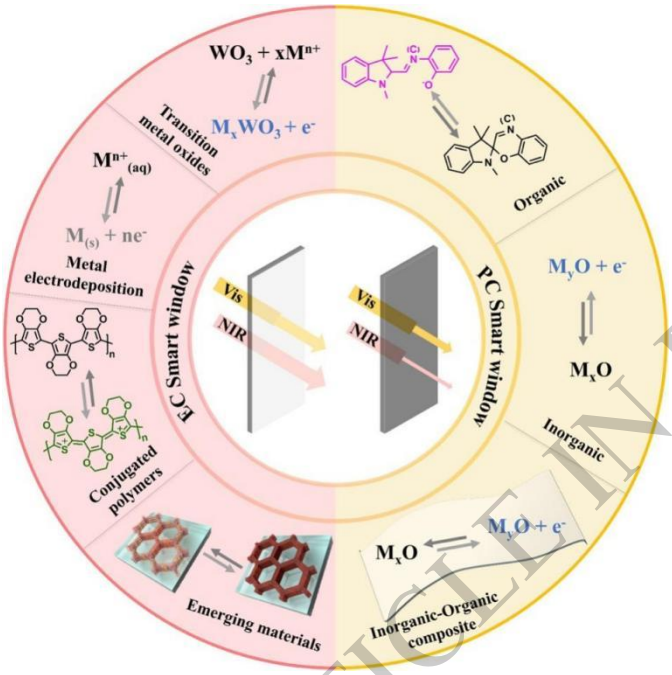


Figure 1. Schematic diagram of the EC smart windows and materials[24]. Copyright © 2025 Wiley-VCH GmbH.

ARTICLE IN PRESS

Notably, electrochromic devices share strong similarities in material selection, device architecture, and reaction kinetics, as their optical modulation generally relies on reversible ion intercalation/deintercalation or surface redox reactions[25,26]. This underlying commonality provides a foundation for engineering multiple electrochemical processes within a single-component electrochromic material, thereby enabling independent spectral modulation across different wavelength bands and paving the way for advanced dual-band electrochromic smart windows[27,28]. To clearly define and illustrate the concept of dual-band electrochromism, **Figure 1** presents a

schematic overview comparing traditional single-band and advanced dual-band electrochromic smart windows. Unlike conventional systems that simultaneously modulate both visible (VIS) and near-infrared (NIR) regions, dual-band electrochromic materials (encompassing transition metal oxides, conducting polymers, and emerging composite systems) offer the unique capability to selectively and independently control the transmission of visible light and solar heat (NIR). As depicted in the central diagram, this technology enables multi-state optical regulation-such as maintaining high transparency for visible light while blocking NIR heat, or simultaneously attenuating both bands-thereby providing advanced energy-saving solutions for smart buildings and automotive applications. In recent years, researchers have demonstrated efficient dual-band electrochromism across a diverse range of single-component material systems, including doped or non-stoichiometric titanium oxides, tungsten oxide nanocrystals and nanowires, niobium–tungsten oxides, and conducting polymers[29]. By exploiting mechanisms such as localized surface plasmon resonance, polaron absorption, and band-edge transitions, these materials enable single-component architectures with multistate optical switching and tunable VIS/NIR modulation. The combination of distinct optical mechanisms within a single material can facilitate spectral decoupling, while several systems exhibit excellent cycling stability exceeding 10,000 cycles, underscoring their potential for durable dual-band electrochromic applications.

ARTICLE IN PRESS

Nevertheless, despite the remarkable progress achieved in single-component dual-band electrochromic materials, the field continues to confront several critical challenges: scalable synthesis protocols remain predominantly confined to lab-scale batches, hindering commercial viability; issues concerning spatial uniformity and electric field distribution in large-area devices have yet to be fully resolved; and although cycling stability has incrementally improved, a substantial gap persists between current metrics and the tens of thousands of cycles demanded by industrial manufacturing[30]. Furthermore, the synergistic mechanisms governing the integration of electrochromic and energy storage functions within the same material system

require deeper elucidation. Specifically, an intrinsic contradiction exists in their charge-density requirements: high-performance electrochromism demands high optical density modulation at low charge densities, whereas energy storage seeks high charge densities, thereby introducing additional complexity to material design[31,32].

This review systematically summarizes the recent advances in single-component dual-band electrochromic materials and devices, with a particular focus on material design strategies, underlying modulation mechanisms, device architectures, and application prospects. We first introduce the fundamental principles and key performance metrics of dual-band electrochromism, followed by a comprehensive discussion of material design strategies and the corresponding mechanisms for decoupling visible and near-infrared optical modulation in inorganic and organic systems. We then summarize recent progress in device fabrication and multifunctional applications, particularly for smart windows and adaptive optical management. Finally, the remaining challenges and future development directions are discussed, with the aim of providing insights into the rational design and practical implementation of high-performance single-component dual-band electrochromic devices.

ARTICLE IN PRESS

2.Principles and Evaluation Metrics of Dual-Band Electrochromism

2.1 Principle

Researchers have proposed several different mechanism models to explain the electrochromic phenomenon. Currently, most researchers agree on the double injection model[33].

The double injection model, also known as the Faughnan model or valence charge transfer model, was proposed by Faughnan in 1975. Taking the typical electrochromic material WO_3 as an example, the electrochromic mechanism according to this model can be expressed as:

$$WO_3 + xe^- + xA^+ \rightleftarrows A_xWO_3$$

In the A+ formula, small ions such as Li^+, Na^+, and H^+ are involved. When a negative potential is applied, electrons and cations combine and become embedded in the WO_3 matrix, resulting in the formation of a blue tungsten bronze compound. Consequently, WO_3 changes its color from colorless to blue. Conversely, when a positive potential is applied, electrons and cations are jointly removed from the WO_3 matrix, causing the disappearance of the tungsten bronze compound and leading to the color change of WO_3 from blue to colorless.

2.2 Performance Metrics

2.2.1 Optical Modulation Amplitude

Light modulation amplitude refers to the change in light transmittance or absorbance at a specific wavelength between the colored state and the faded state. It is a crucial parameter for evaluating excellent electrochromic performance. The desired optical modulation range is 100%, where the material is completely opaque in the tinted state and completely transparent in the faded state. The amplitude of light modulation is determined by the change in transmittance (ΔT, also commonly referred to as optical contrast) or absorbance (ΔA, also referred to as absorbance contrast) of an electrochromic material or device at a specific wavelength, which can be calculated using the following equation:

$$\Delta T = T_{colored} - T_{bleached}$$

ARTICLE IN PRESS

Given the selective modulation of visible light and near-infrared light by dual-band electrochromic materials, it is expected that electrochromic materials or devices exhibit a significant light modulation amplitude. Among the various electrochromic materials reported to date, the optical modulation can reach as high as 97.7%[34].

2.2.2 Response time

The response time refers to the time it takes for the electrochromic material to change from the colored state to the faded state (T_b) or from the faded state to the colored state (T_c). This time is typically measured as the duration required for a 90% change

in the optical modulation range. The response time is influenced by factors such as the electronic conductivity of the electrode, the ionic conductivity of the electrolyte, and the ion diffusion process within the device. Additionally, the device's structure, the morphology of the electrochromic material, and the applied voltage scheme have a significant impact on the response time. Different application scenarios have varying requirements for response time. Although users cannot directly perceive infrared transmittance and its related response time in practical applications, color changes usually accompany infrared blocking, and excessively slow switching speeds can also affect device performance. For instance, in display applications, extremely short switching times are essential. On the other hand, longer switching times can be tolerated in smart glasses applications.

2.2.3 Coloration efficiency

Coloring efficiency (CE) is defined as the change in transmittance or absorbance per unit area at a given wavelength due to the injected charge. Measuring the power consumption of electrochromic devices during the fading transition process is a crucial metric. Higher electron consumption efficiency results from higher coloring efficiency, which is determined using the formula.

$$CE=\frac{\Delta A}{Qd}=\frac{\log(\frac{T_{bleached}}{T_{colored}})}{Qd}$$

ΔA can be converted into a change in transmittance according to Bill Lambert's law, Qd is the charge density ($cm^2\ C^{-1}$), Tbleached is the transmittance of the faded state, Tcolored is the transmittance of the colored state, and the unit of CE is $cm^2\ C^{-1}$.

2.2.4 Bistability

The term “bistability” describes an electrochromic device's capacity to hold onto its color when it is in the open circuit condition. This property, sometimes referred to as the memory effect, allows electrochromic devices to hold their stability even when the external voltage is withdrawn, whether they are colored or faded. Electrochromic

ARTICLE IN PRESS

devices do not always require power to maintain the desired optical properties, in contrast to other electronic devices like light-emitting diodes (LEDs), organic light-emitting diodes (OLEDs), or liquid crystal displays (LCDs), which require continuous power to maintain a display state. In order to stabilize the electrochemical reduction/oxidation state of the electroactive materials inside the device and achieve optimal memory effects, highly complicated device structure designs are typically required. For instance, the auto fading of liquid electrochromic devices occurs when the electroactive components spread and readily exchange electrons inside the device, causing the color to fade quickly even in the absence of an applied voltage. Because self-fading processes are avoided and the diffusion of electroactive components is restricted, solid and semi-solid devices typically display higher bistability.

Because no additional voltage is required, good bistable behavior can lower energy usage. This has a big impact on the practical use of electrochromic smart windows in energy conservation.

ARTICLE IN PRESS

2.2.5 Cycling stability

Cycle stability, which is often determined by counting the number of electrochemical oxidation-reductions an electrochromic device experiences before its optical modulation range falls to a specific percent, is a good indicator of the device's service life. A key component of superior electrochemical performance is the materials' ability to remain stable over redox cycles. Furthermore, the device cycle stability is more influenced by the applied voltage, ambient factors, and device structure. The primary barrier to the continued development of the majority of electrochromic devices is the requirement for the device to retain stable fading performance beyond 10^4 cycles in practical applications[35]. Durability is a crucial factor that decides whether an electrochromic device can be utilized, along with cycling stability. For a number of years, electrochromic devices that meet the necessary requirements should function well. Electrochromic devices are frequently sealed to prevent the negative effects of air and water in the external environment, improving long-term stability and

endurance. The stability of electrochromic devices can also be preserved by using an appropriate voltage scheme and a sensible blend of electroactive materials.

3.Single-Component Dual-Band Electrochromic Material Systems

Architectural windows serve as the most active interfaces for energy exchange between indoor and outdoor environments[3]. Within solar radiation, visible light (VIS, 380-780 nm) carries only about 45% of the energy yet entirely dictates natural daylighting and visual clarity, whereas near-infrared light (NIR, 780-2,500 nm) accounts for approximately 50% of the energy and acts as the primary source of indoor heat gain [36, 37]. Human demands for light and heat are frequently asynchronous across different seasons and times of day: at noon in summer, there is a dual need to block scorching NIR radiation to mitigate air-conditioning loads while maintaining adequate visible light transmission to avoid lighting energy consumption, whereas on winter days, the goal is to maximize NIR collection for auxiliary heating while preserving a bright field of view. For conventional inorganic electrochromic materials (e.g., amorphous WO_3), visible and near-infrared absorption increase or decrease almost synchronously during ion intercalation, restricting windows to a binary toggle between fully transparent and heavily darkened/insulated states and rendering them incapable of meeting such complex multi-scenario modulation requirements[38,39]. The ultimate objective of dual-band independent modulation is to achieve asynchronous, reversible, and voltage-selective control over the visible transmittance (T-VIS) and near-infrared transmittance (T-NIR)[40], thereby engineering four distinct, ideal optical states on a single-component electrochromic electrode[41]: a bright state (high T-VIS/high T-NIR) that admits winter daylight and solar heat; a cool state (high T-VIS/low T-NIR) that selectively blocks near-infrared heat while preserving a clear view, aligning with summer daytime energy-saving requirements; a dark state (low T-VIS/ high T-NIR) capable of harvesting partial solar heat under glare-prevention or privacy-demanding scenarios; and a fully blocked state (low T-VIS/low T-NIR) designated for extremely hot or complete shading conditions. These four states occupy the four vertices of an ideal rectangle in the T-VIS/T-NIR phase space; the

ARTICLE IN PRESS

closer a material can approach these vertices, the stronger its dual-band independent modulation capability becomes. The physical foundation underlying this concept relies on the material possessing two distinctly separated electrochemical potential windows, which are coupled with spectrally discrete near-infrared and visible absorption channels, respectively. The ideal spectral evolution process unfolds as follows: under a low-voltage first-stage modulation, the near-infrared transmittance decreases significantly due to small polaron absorption or localized surface plasmon resonance induced by shallow ion intercalation, while the visible transmittance remains largely unaffected; upon applying a higher voltage, deep-level intercalation or structural phase transition triggers intense visible absorption, whereas the near-infrared region remains blocked or undergoes further attenuation, demonstrating a distinct asynchronous relationship between the two modulations in terms of potential.

Researchers have developed a variety of pathways to achieve independent dual-band modulation, focusing on both single-component and combinatorial strategies. **Figure 2**a schematically depicts the practical application of smart windows, highlighting their capability to selectively manage solar light (visible) and heat (NIR) for indoor thermal comfort and energy efficiency (**Figure 2**a). For instance, Chen et al. prepared oxygen-vacancy-rich amorphous tungsten oxide (a-WO_{3-x}-OV) thin films via electron-beam evaporation in a hypoxic atmosphere; leveraging localized surface plasmon resonance induced by oxygen vacancies, these films selectively absorb near-infrared light at low voltages without sacrificing visible light transmittance, while the oxygen vacancies provide abundant ion diffusion channels to enable seamless switching among "bright", "cool", and "warm" modes, thereby substantially enhancing electrochromic perform(**Figure 2**b,c and d). To address the limited optical contrast and modulation range of colored materials, Jia et al.[42] introduced a Li^+/Al^{3+} composite solid electrolyte into a VO_2/WO_3 electro-thermo dual-responsive device; through ionic synergetic effects, this design effectively regulates the phase transition of VO_2 and enhances the color-changing capability of WO_3, achieving four-state switching with a cycling stability exceeding 10,000 cycles (**Figure 2**e). Additionally, Ma et al. [43]

ARTICLE IN PRESS

prepared a $Ce_4W_9O_{33}$ electrode based on zinc-ion electrochemical activity that intrinsically exhibits three optical states: a “bright-warm” state with dual transparency in both visible and near-infrared regions, a dual-opaque “dark-cool” state, and a “bright-cool” state that is transparent to visible light yet opaque to near-infrared light (**Figure 2**f). When assembled with a NiO counter electrode and a zinc anode to form a complementary device, a "dark-warm" state-opaque to visible light but transparent to near-infrared light-was further introduced, thereby achieving dual-band independent regulation across four distinct modes and demonstrating exceptional potential for solar radiation modulation (**Figure 2**g), which offers an effective strategy for electrochromic windows to intelligently adapt to climatic conditions and personal preferences.

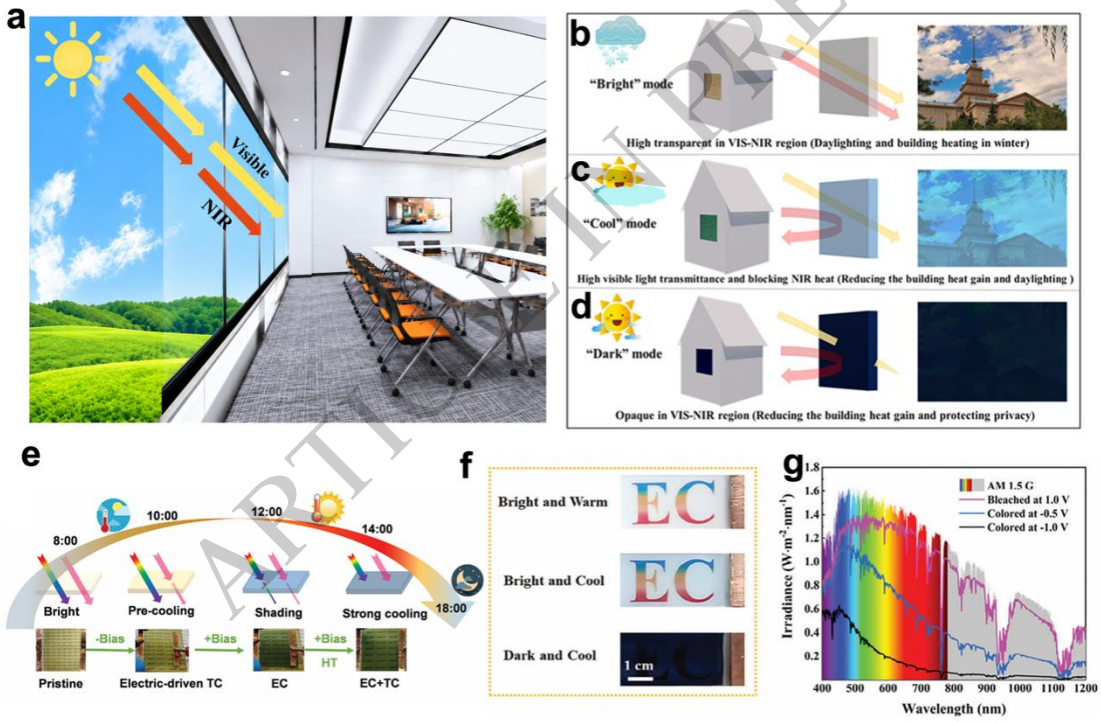


Figure 2. (a)Schematic illustration of a smart window dynamically regulating visible light and NIR radiation in a building. Application scenarios of the DEES window in (b) bright, (c) cool and (d) dark operating modes[44]; Copyright © 2023 The Royal Society of Chemistry. (e) dynamic dimming modes of Li^+/Al^{3+} base electric-thermal dual responsive devices[42]; Copyright © 2022 Wiley-VCH GmbH. (f) Digital photographs, and (g) solar irradiance spectra of the $Ce_4W_9O_{33}$ film electrode at different states[43]. Copyright © 2024 Wiley-VCH GmbH.

ARTICLE IN PRESS

To provide a clear and consolidated physical and chemical picture of asynchronous visible (VIS) and near-infrared (NIR) optical switching, Table 1 systematically summarizes representative single-component materials along with their underlying decoupling mechanisms, operational redox transitions, and primary spectral response ranges. As categorized in the summary, inorganic systems primarily operate through electrochemically induced oxygen-vacancy modulation, localized surface plasmon resonance (LSPR) frequency tuning, and small-polaron hopping (or intervalence charge transfer), which enable continuous NIR attenuation prior to significant VIS state transitions. Conversely, organic platforms-including conjugated polymers, viologens, and electroactive framework architectures-rely on multi-stage redox dynamics and progressive polaron-bipolaron (radical cation to dication) evolutions. These discrete molecular orbital reconfigurations allow distinct NIR absorption bands to be triggered independently of VIS coloration.

Table 1. Classification of single-component dual-band electrochromic materials and their corresponding optical decoupling mechanisms.

Material Class	Representative Materials	Key Decoupling Mechanism	Active Redox States/Transitions	Primary Spectral Modulation
Inorganic	DefectiveWO_{3-x}, $W_{18}O_{49}$	Oxygen vacancies& Small-polaron hopping	W^{6+}/W^{5+} (charge transfer)	Independent NIR absorption via polaron absorption; VIS color change at high intercalation

ARTICLE IN PRESS

Inorganic	Doped metal oxides (e.g., FTO, ITO,Nb_2O_5)	LSPR frequency tuning & Free-carrier pumping	Reversible ion injection changing free-carrier density (n_e)	Selective NIR modulation via LSPR shift without disturbing VIS transparency
Organic	Conjugated polymers (e.g., PEDOT, PBFDO/n-PBDF)	Stepwise redox & Polaron-bipolaron evolution	Neutral Polaron (P^+/P^-) Bipolaron (P^{2+}/P^{2-})	Polaron state induces strong NIR absorption; Bipolaron/neutral shift governs VIS attenuation
Organic	Viologen derivatives & Small molecules	Multi-stage electron transfer & Radical species	$V^{2+}/V^+/V^0$	V^+ radical generates dual VIS/NIR bands; multi-stage redox decouples bands
Organic	Electroactive Polyimides / Frameworks (COFs/MOFs)	Localized charge transfer & IVCT / Radical delocalization	Stepwise oxidation of triarylamine /carbazole units	Radical cation generation enables discrete NIR intervalence bands prior to VIS shifts

ARTICLE IN PRESS

3.1 Inorganic Single-Component Dual-Band Electrochromic Materials

Inorganic single-component dual-band electrochromic materials enable the independent regulation of visible and near-infrared light transmittances within a single electrode, the key to which lies in the presence of two or more redox processes with distinct electrochemical potentials that separately couple with optical absorption channels across different spectral bands[45]. Synthetic strategies play a more

fundamental role in this field than is commonly appreciated, enabling intelligent dual-band regulation through precise control over oxygen-vacancy concentrations, structural water content, pre-intercalated ion occupancy, and nano structural morphology.

From the perspective of synthesis, inorganic single-component dual-band electrochromic materials are engineered through tailored fabrication strategies to establish two electrochemical redox processes with distinct potentials within a single material, each selectively coupled to visible and near-infrared absorption channels. Although different synthetic routes emphasize distinct mechanisms for achieving this objective, they collectively underscore the intrinsic relationship among processing parameters, structural characteristics, and optical responses. Physical deposition under oxygen-deficient or reducing atmospheres represents the most direct route for tailoring the stoichiometry of transition-metal oxides[46, 47]. Taking amorphous tungsten oxide as an example, decreasing the oxygen partial pressure during electron-beam evaporation or magnetron sputtering markedly increases the concentration of oxygen vacancies within the film, accompanied by the partial reduction of W^{6+} to W^{5+} or even W^{4+} and a concomitant increase in free-carrier density[48, 49]. This compositional change optically activates two distinct near-infrared absorption mechanisms-localized surface plasmon resonance and small-polaron hopping-allowing the film to preferentially attenuate near-infrared radiation even at low voltages, whereas visible-light absorption is activated only at higher degrees of ion intercalation[50-52]. Meanwhile, oxygen vacancies provide more abundant diffusion pathways and binding sites for Li^+ or H^+, substantially improving ion-insertion kinetics and thereby simultaneously enhancing optical selectivity and electrochromic performance. Building on this overarching concept, different research groups have explored diverse synthetic strategies tailored to specific fabrication techniques[41].

Chen et al. [21] fabricated orthorhombic oxygen-deficient tungsten oxide (o-WO_{3-x}) films (**Figure 3**a) by post-annealing electron-beam-evaporated films in an Ar

ARTICLE IN PRESS

atmosphere. In contrast to stoichiometric tungsten oxide (s-WO_3), which exhibits an irregular and densely packed island-like surface morphology, the o-WO_{3-x} films possess a porous architecture composed of uniformly distributed nanoparticles, facilitating electrolyte infiltration and rapid ion insertion. Moreover, the abundant oxygen vacancies enable the films to maintain stable dual-band electrochromic performance even in acidic aqueous electrolytes (**Figure 3**b). The resulting all-solid-state inorganic dual-band electrochromic device selectively modulates visible and near-infrared transmittance with excellent overall performance, demonstrating the practical value of synergistically integrating oxygen-vacancy engineering and porous morphology in the design of single-component inorganic dual-band electrochromic materials. Wet-chemical doping provides an effective avenue for introducing electrochemically active sites while preserving the host crystal framework . Li et al. [53] synthesized titanium-containing tungsten-molybdenum oxide (Mo/Ti:WO, MTWO) colloids via a wet-chemical method involving sequential ion exchange of Ti^{4+} with W^{6+}/Mo^{6+}. The doping process introduced additional cation vacancies that serve as intercalation sites for zinc ions, thereby unlocking the electrochemical activity of the material toward Zn^{2+}. Concurrently, doping significantly reduced the particle size, causing MTWO to exhibit an ultrafine nanowire morphology; this not only enhanced electrolyte accessibility but also shortened internal ion diffusion distances (**Figure 3**c-h). Consequently, compared to pristine WO_3, MTWO leverages randomly distributed cation vacancies more effectively for zinc-ion storage, ultimately achieving higher charge capacity and superior optical contrast. Furthermore, Zhao et al. [54] reported a spectrally selective dual-band electrochromic smart window that dynamically regulates solar irradiance to balance indoor daylighting and thermal management. As a representative dual-band optical modulation platform, hexagonal cesium-doped tungsten bronze (h-$Cs_{0.32}WO_3$, CWO) nanocrystals synthesized via a one-pot method offer an attractive structural framework (**Figure 3**i). Structural and morphological characterizations confirm the formation of the hexagonal phase, with the resulting nanosheets exhibiting a fine lateral dimension under 30 nm; these well-dispersed nanocrystals form highly stable colloidal suspensions that display a distinct Tyndall

ARTICLE IN PRESS

effect (**Figure 3**j). In-depth crystallographic analysis reveals that the hexagonal phase features an ordered, hierarchical tunnel network assembled from corner-sharing WO_6 octahedra (**Figure 3**k). These spacious multi-tunnel cavities not only facilitate H^+/e^- co-transport but are also large enough to accommodate the reversible insertion of multi-valence cations such as Li^+ and Al^{3+}, laying the structural foundation for dynamic localized surface plasmon resonance (LSPR) tuning in the near-infrared (NIR) region-distinct from mid-infrared (MIR) thermal emittance modulation mechanisms. Furthermore, the combination of 2D nanosheet crystallographic anisotropy and 1D intragranular tunnel diffusion pathways synergistically accelerates ion transport kinetics, significantly enhancing both the charge capacity and optical modulation capabilities of the material. In the realm of morphological engineering, Cai et al.[45] fabricated ordered nano helical WO_3 (NH-WO_3) films featuring an amorphous heterophase structure (**Figure 3**l). The film achieves independent modulation of visible/near-infrared transmittance and mid-/long-wave infrared emissivity (**Figure 3**m); exhibiting high optical contrast, rapid switching kinetics, and superior durability (**Figure 3**n), it offers a novel design paradigm for next-generation energy-efficient buildings and adaptive optical systems.

Overall, these strategies aim to achieve the potential-dependent decoupling of visible and near-infrared absorption within a single inorganic material. In WO_{3-x} and MoO_{3-x} derived from oxygen-deficient deposition or reductive annealing, oxygen vacancies functioning as shallow donors enable the electrochemical separation of interband charge-transfer absorption (visible region) at low potentials from localized surface plasmon resonance absorption (near-infrared region) at high potentials, thereby establishing a dual-band modulation window[55, 56]. Wet-chemical ion exchange, such as substituting Cs^+ or NH_4^+ in the tunnels of hexagonal WO_3 with K^+ or Li^+, introduces cation vacancies while preserving the tunnel framework, including the triangular, hexagonal, and *c*-axis-aligned square channels. Injected electrons preferentially populate the conduction band or vacancy-associated states prior to occupying the LSPR state, resulting in a stepwise response characterized by a delayed

ARTICLE IN PRESS

onset of near-infrared absorption[57]. Morphological engineering, on the other hand, shortens ion diffusion pathways and enlarges the electrochemically active surface area via mesoporous, nanosheet, or helical hierarchical structures, thereby enhancing ion transport kinetics and the amplitude of dual-band optical modulation. Future work should synergistically integrate these strategies and employ *in situ* UV-VIS-NIR spectro electrochemistry, XPS, and Raman spectroscopy to correlate oxygen vacancy concentration, ion occupancy, and LSPR intensity in real time. This will establish structure-property relationships among synthetic routes, defect/morphology features, and stepwise optical responses, thereby advancing single-component inorganic dual-band electrochromic materials from empirical screening to rational design.

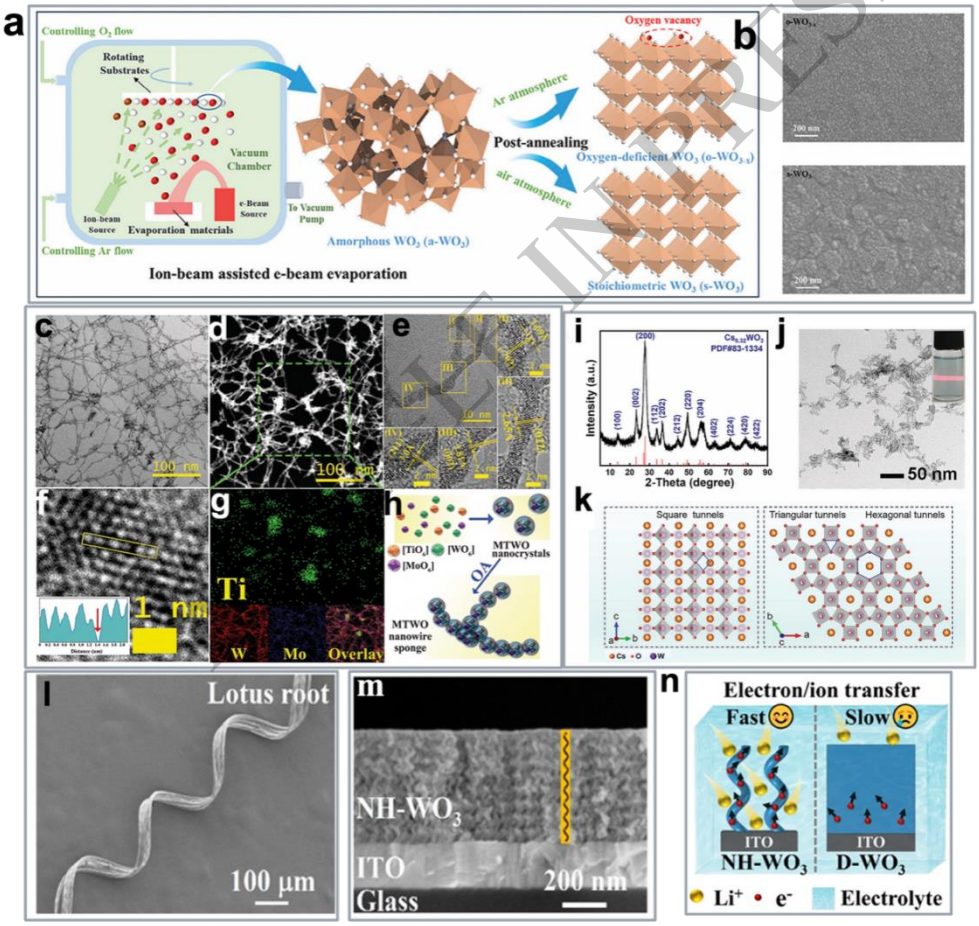


Figure 3. Orthorhombic oxygen-deficient tungsten oxide (o-WO_{3-x}) thin films were fabricated via electron-beam evaporation: (a)chematic diagram of an ion-beam assisted e-beam evaporation method for the preparation of o-WO_{3-x} and s-WO_3 films.(b) Top-view SEM images of the o-WO_{3-x} and s-WO_3 films[21]; Copyright ©

2025 Wiley-VCH GmbH. Characterization of MTWO Prepared via a Wet-Chemical Method：(c) TEM image of the MTWO. (d) DF-STEM image and (e) HR-TEM image of MTWO. (f) Atomic-resolution image of MTWO. The profile plot of a line of atoms (inset), depicting the atomic columns and dark patches in between. The arrow points to the observed cationic vacancy. (g) EDS elemental mapping results for MTWO of the dotted region. (h) Schematic illustration of the formation of nanowire sponges[53]；Copyright © 2019 Wiley-VCH GmbH. Characterization of One-Pot-Synthesized CWO(h-$Cs_{0.32}WO_3$): (i) XRD pattern of the CWO nanoplatelets. (j) TEM image of CWO nanoplatelets. The inset displays a digital photograph of the colloidal solution of CWO, with the Tyndall effect visible under the laser beam. (k) The tunnel structure of hexagonal CWO along the a-axis and c-axis[54]；Copyright © 2024 Wiley-VCH GmbH. Lotus-root-like amorphous heterophase NH-WO_3 films:(l) SEM images of lotus root vessels. (m) SEM images of NH-WO_3. (n) COMSOL multiphysics-based fluid dynamic simulations[45]；Copyright © 2025 The Authors.

3.2 Single-Component Organic Dual-Band Electrochromic Materials

Single-component organic dual-band electrochromic materials represent the most active research frontier and the domain of most significant performance breakthroughs in this field. The central design premise of these materials relies on precise molecular engineering to enable stepwise, reversible redox reactions of a single component across distinct potential windows. Each redox state exhibits characteristic absorption bands focused in the visible and near-infrared regions, respectively, thereby fundamentally decoupling dual-band optical modulation [58-60]. Based on their chemical nature, these materials can be clearly categorized into two major classes: conducting polymers and small organic molecules/metal complexes, each offering distinct advantages in terms of modulation mechanisms and performance characteristics[61, 62]. Nevertheless, fabricating low-cost, high-performance visible-to-near-infrared electrochromic devices remains a highly challenging endeavor [63].

ARTICLE IN PRESS

Lu et al. [64] synthesized a fluorophenyl-modified polythiophenone via a one-step Grignard coupling reaction combined with low-potential electropolymerization, which proceeded continuously at 1.0 V (vs. Ag/AgCl). Leveraging intermolecular hydrogen bonding between the fluorinated polythiophene chains, a dense, self-supporting polymer film was electrodeposited, thereby enhancing both its mechanical strength and electrical conductivity. The resulting polymer film demonstrated exceptional overall electrochromic performance along with facile electropolymerization patterning (**Figure 4**a). Such patterned electrochromic devices exhibit considerable application potential in deformable displays, color-changing e-skin tattoos, and infrared camouflage, while offering stable color switching and robust mechanical properties. Wu et al. [65] introduced a semi-interpenetrating double polymer network (DPN) organogel comprising linear PVDF-HFP and crosslinked VIO-PIL to enhance the cycling stability of viologen-based electrochromic devices (**Figure 4**b). Covalently anchoring the viologen within VIO-PIL suppressed irreversible face-to-face dimerization between radical cations, while the strongly polar –F groups in the linear PVDF-HFP further restricted the viologen moieties via electrostatic interactions and boosted the mechanical properties of the organogel. **Figure 4**c summarizes the performance of electrochromic devices based on various alkenyl viologens (blue, green, and magenta), highlighting their potential for applications in energy-efficient smart windows and wearable electronics.

ARTICLE IN PRESS

Conducting polymers (CPs) represent highly attractive candidates owing to their intrinsic flexibility and electronic conductivity; however, their practical implementation is frequently constrained by poor long-term stability and performance degradation-particularly under thermal or mechanical stress-which stems primarily from structural degradation and over-oxidation at high potentials[66, 67]. To address these challenges, Lin et al.[68] proposed a dual-strategy molecular design combining deuterium substitution with Lewis acid-assisted polymerization to intrinsically stabilize poly(3,4-ethylenedioxythiophene) (PEDOT), thereby suppressing backbone

vibrational energy and mitigating over-oxidation degradation during redox cycling. In this approach, replacing hydrogen atoms with heavier deuterium (D) atoms lowers the stretching vibration frequency of C─D bonds in the polymer chains, enhancing molecular rigidity and structural elasticity, which reduces vibrational energy and reinforces backbone stability along with operational electrochemical performance (**Figure 4**d). The resulting PEDOT-D films fabricated via this strategy exhibit outstanding multifunctional performance, and the integrated wearable electrochromic supercapacitors similarly demonstrate exceptional performance, providing a rational design blueprint for developing mechanically robust, thermally adaptive, and optically responsive next-generation flexible energy systems.

Polyaniline (PANI)-based infrared electrochromic devices (IR-ECDs) feature advantages such as broad spectral response ranges and multi-state tunability; however, devices prepared via conventional solution-processing methods often suffer from limited infrared radiation modulation capability, poor mechanical stability, and insufficient scalability, severely hindering their practical implementation [69, 70]. To address these challenges, Li et al.[71] proposed a scalable fabrication strategy centered on a bicontinuous "electron-ion" transport network. By growing PANI *in situ* on the surfaces of template-acidified carbon nanotubes (CNTs), interfacial molecular ordering was successfully achieved (**Figure 4**e). In this architecture, the CNTs serve as both efficient charge transport channels for PANI and reservoirs for protons. The incorporation of CNTs significantly boosted carrier mobility and the utilization efficiency of polarons/bipolarons, thereby markedly enhancing the infrared radiation modulation capability of the device while imparting high redox activity and excellent reversibility to the system. Furthermore, by mounting the IR-ECD onto the trailer of a scale-model truck and applying external voltages, the researchers achieved real-time dynamic modulation of surface thermal radiation (**Figure 4**f). This work offers a versatile and scalable solution for constructing next-generation PANI-based infrared electrochromic devices, demonstrating exceptional modulation authority, durability, and application adaptability for advanced thermal management systems.

ARTICLE IN PRESS

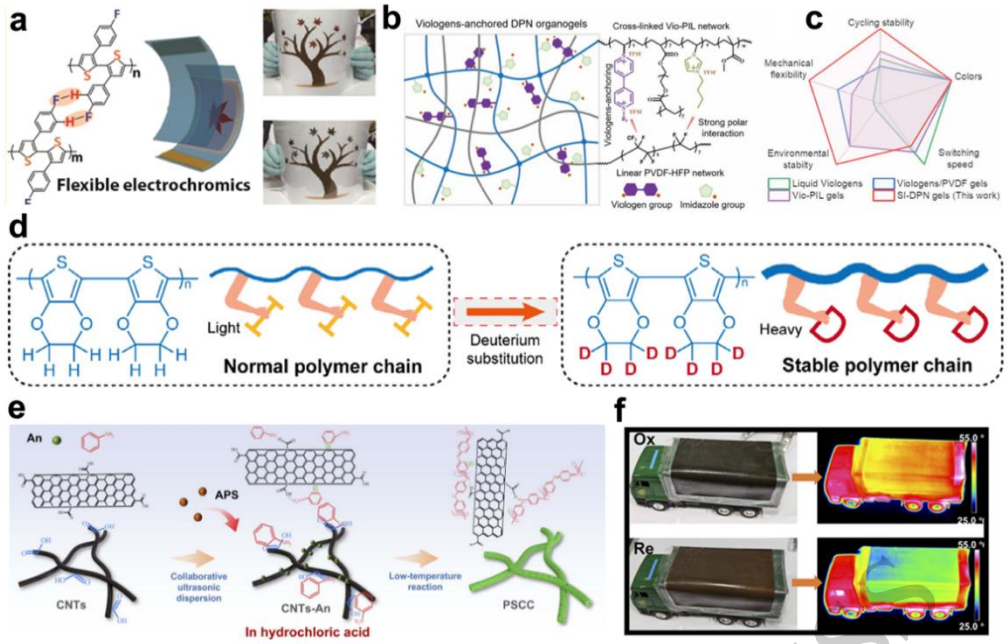


Figure 4. Organic Single-Component Dual-Band Electrochromic Materials: (a) Reversible color changes under bending[64]; (b)Synergistic molecular confinement via viologen anchoring and polar interaction. (c) Schematic illustration of the semi-interpenetrating DPN organogels. Copyright © 2022 American Chemical Society. (d) Radar chart for comparison of cycling stability, colors, switching speed, environmental stability, and mechanical flexibility among the viologens-based EC electrolytes[65]； Copyright © 2023 Wiley-VCH GmbH. C─D bond-induced strengthening of the PEDOT-D backbone[68]:(e) In situ PANI coating on CNTs； Copyright © 2026 Wiley-VCH GmbH. (f) IR thermal images of oxidation and reduction states on a heated car model[71]； Copyright © 2026 The Royal Society of Chemistry.

ARTICLE IN PRESS

Beyond classic conjugated polymers (e.g., PEDOT, PANI) and viologens, a diverse array of alternative organic and organic–inorganic hybrid systems have emerged to achieve single-component dual-band electrochromism through distinct redox mechanisms and tailored molecular architectures. For instance, small-molecule chromophores (such as triphenylamine derivatives) and transition metal complexes offer highly discrete molecular orbital tuning; upon stepwise oxidation or reduction, they undergo reversible intervalence charge transfer (IVCT) or ligand-to-metal charge

transfer (LMCT), enabling precise and independent optical modulation across the VIS and NIR regions[72, 73]. Moving to framework materials, covalent organic frameworks (COFs) and metal–organic frameworks (MOFs) incorporate redox-active linkers or functional chromophores within highly ordered crystalline networks, where permanent porosity accelerates ion transport while radical generation and spatial charge delocalization foster decoupled dual-band optical switching[74, 75]. Similarly, coordination frameworks based on Prussian blue analogues (PBAs) capitalize on reversible multi-electron mixed-valence transitions (e.g., Fe^{II}/Fe^{III}) or metal-to-ligand charge transfer), giving rise to intense NIR intervalence absorption alongside distinct visible coloration[76]. Furthermore, electroactive polyimides and non-conjugated polymers embedded with redox-active pendant groups-such as triarylamine or carbazole moieties-combine superior thermal and mechanical stability with clear multi-stage redox dynamics, operating via localized charge-transfer mechanisms that effectively decouple VIS and NIR optical responses without requiring extended backbone conjugation[77].

ARTICLE IN PRESS

4.Applications of Single-Component Dual-Band Electrochromic Devices

The paramount application value of single-component dual-band electrochromic materials lies in their ability to achieve asynchronous modulation of visible and near-infrared light on a single electrode without requiring complex multilayer heterostructures, offering intrinsic advantages for simplifying device architectures, reducing manufacturing costs, and enhancing long-term stability[78, 79]. At the device level, researchers typically assemble the single-component electrochromic layer with transparent conductive substrates[80, 81], an ion storage layer, and an electrolyte into a sandwich-type structure, wherein programmed applied voltages direct ion insertion/extraction or redox reactions to achieve switching among various optical states, including “bright-warm”,“bright-cool”, “dark-warm”, and “dark-cool”[82-84]. In this section, we highlight the application scenarios of single-component dual-band electrochromic devices. Furthermore, to provide a broader technological perspective, we also discuss extended application horizons-including complementary cell designs,

multi-band integration, and energy-storage coupling-as futuristic outlooks for smart windows.

Growing public concern over energy and environmental issues has driven an increasing market demand for energy-efficient and environmentally friendly devices [85, 86]. Electrochromic devices can reversibly and persistently alter their optical properties under a small electric field, attracting widespread attention due to their promising application prospects in smart windows, energy-efficient displays, switchable mirrors, camouflage, and other cutting-edge fields (**Figure 5**)[81]. However, electrochromic smart windows serve as the most commercially promising application platform for single-component dual-band materials. Approximately 30%-40% of building energy consumption stems from space heating, cooling, and artificial lighting; as the most dynamic component for energy exchange within the building envelope, windows directly dictate the indoor optical-thermal environment and overall energy consumption through their spectral regulation capability. Conventional electrochromic smart windows typically only allow broadband, simultaneous modulation of visible and near-infrared light-switching strictly between fully transparent and fully darkened states-thus failing to meet the distinct seasonal and diurnal demands for daylighting and solar heat gain [87]. Single-component dual-band electrochromic materials achieve asynchronous modulation of visible and near-infrared transmittance within a single electrode, enabling smart windows to reversibly switch among multiple optical states, such as “bright-warm”, “bright-cool”, “dark-warm” and “dark-cool”; this maximizes the utilization or blockage of solar thermal radiation while ensuring visual comfort, thereby significantly reducing HVAC and lighting energy consumption[88, 89].

In practical device construction, researchers typically utilize a single-component electrochromic film as the working electrode, assembled with a transparent conductive substrate, an ion storage layer, and an electrolyte into a sandwich structure, controlling the depth of ion intercalation/deintercalation or redox reactions

ARTICLE IN PRESS

via voltage programming to achieve reversible switching among multiple optical states (**Figure 5**b, c and d). Currently, various single-component inorganic and organic material systems have been successfully employed in dual-band smart window prototypes, demonstrating high optical modulation amplitudes and good cycling stability in both the visible and near-infrared regions[90].

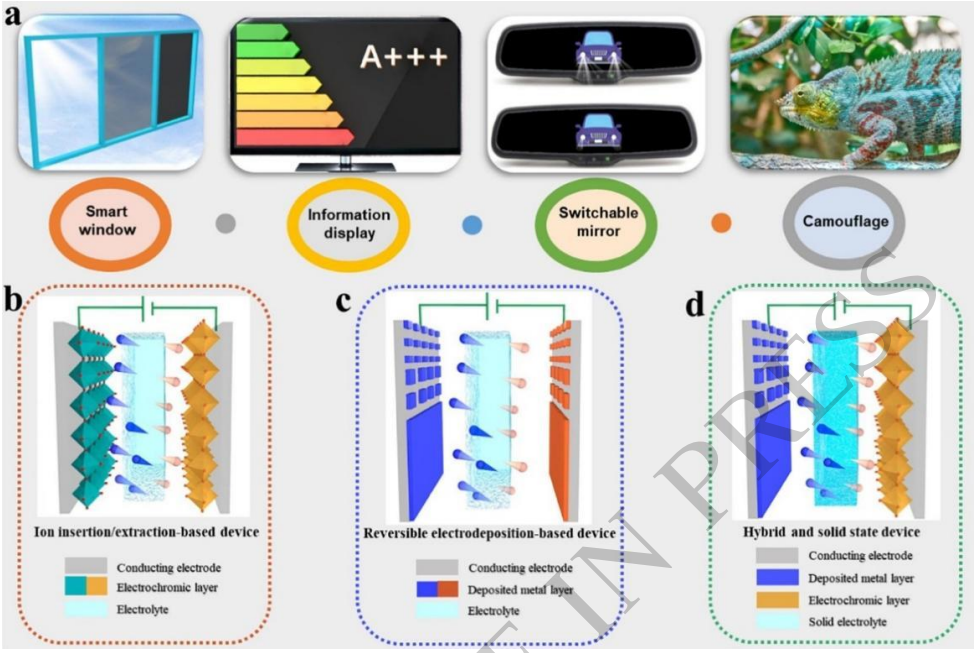


Figure 5. Applications and Device Architectures of Electrochromics[81]. Copyright © 2025 Elsevier Ltd.

ARTICLE IN PRESS

From the perspective of practical application performance, the energy-saving benefits of single-component dual-band smart windows primarily stem from their decoupled management of visible and near-infrared energy across the solar spectrum [91]. During summer days, the window switches to the “bright-cool” mode, maintaining high visible light transmittance to meet daylighting needs while substantially blocking near-infrared radiation to reduce solar heat gain and lower air-conditioning cooling loads; in winter, it switches to the “bright-warm” mode, harvesting near-infrared heat to assist indoor heating and reduce heating energy consumption [92]. Furthermore, certain devices provide additional benefits for localized building self-powering through charge storage during the coloring process and electrical energy release during bleaching . At the building integration level, scaling up dimensions, achieving

mechanical flexibility, and lowering driving voltages constitute the critical challenges for realizing large-scale applications [93].

For instance, Zhang et al. [94] reported a high-performance dual-band electrochromic device utilizing a tungsten oxide quantum dot (WO_3-QD) cathode and a zinc anode (**Figure 6**a). By elucidating the charge transfer mechanism during zinc ion intercalation/deintercalation, they achieved independent modulation of visible and near-infrared light across three distinct modes (bright, cool, and dark) (**Figure 6**b), exhibiting optical modulation amplitudes of 78.8% and 57.0% at 633 nm and 1200 nm, respectively (**Figure 6**c). Upon switching to the cool mode (0.75 V), the ZDED can block 68.0% of solar heat from entering the building while simultaneously providing a visible light transmittance of up to 62.1% for natural daylighting (**Figure 6**d). Consequently, dynamic switching among these operational states enables a substantial reduction in energy consumption.In addition, Zhang et al.[95] developed a multi-band electrochromic smart window (MESW) with a BaF_2/WO_{3-x}/ITO/electrolyte/Zn/glass/ITO configuration (**Figure 6**e), enabling simultaneous modulation of visible-NIR transmittance and MIR emissivity across bright-heating, bright-cooling, and dark-cooling states (**Figure 6**f,g). EnergyPlus simulations showed that the optimized MESW reduced annual energy consumption by 10.7% compared with commercial low-e glass in Nanjing, China (**Figure 6**h and **Figure 6**i), with a maximum annual energy saving of 141.2 MJ m^{-2} in Accra, Ghana under global climatic conditions (**Figure 6**j). These results demonstrate the potential of multi-band electrochromic windows for dynamic solar and thermal management and energy-efficient buildings. Regarding organic systems, Cao et al.[96] reported the first robust and stable dual-band electrochromic smart window based on single-component polyaniline(**Figure 6**k), which leverages progressive electrochemical reactions to independently modulate near-infrared and visible light transmittances while simultaneously achieving multicolor switching among yellow, green, and black states, delivering optical modulation amplitudes of 65% at 633 nm and 59% at 1600 nm, respectively (**Figure 6**l). The PANI-based DESW device exhibits light yellow, green,

ARTICLE IN PRESS

and deep blue colors in the ‘‘bright’’, ‘‘cool’’, and ‘‘dark’’ modes, respectively. Thermal imaging shows corresponding absorber-plate temperatures of 43.2, 31.8, and 27.2 °C, confirming distinct thermal regulation among the three optical states (**Figure 6**m). The robust and stable multicolor-tunable DESW devices address the limited availability of colorful dual-band smart windows and hold considerable promise for energy-efficient building applications.

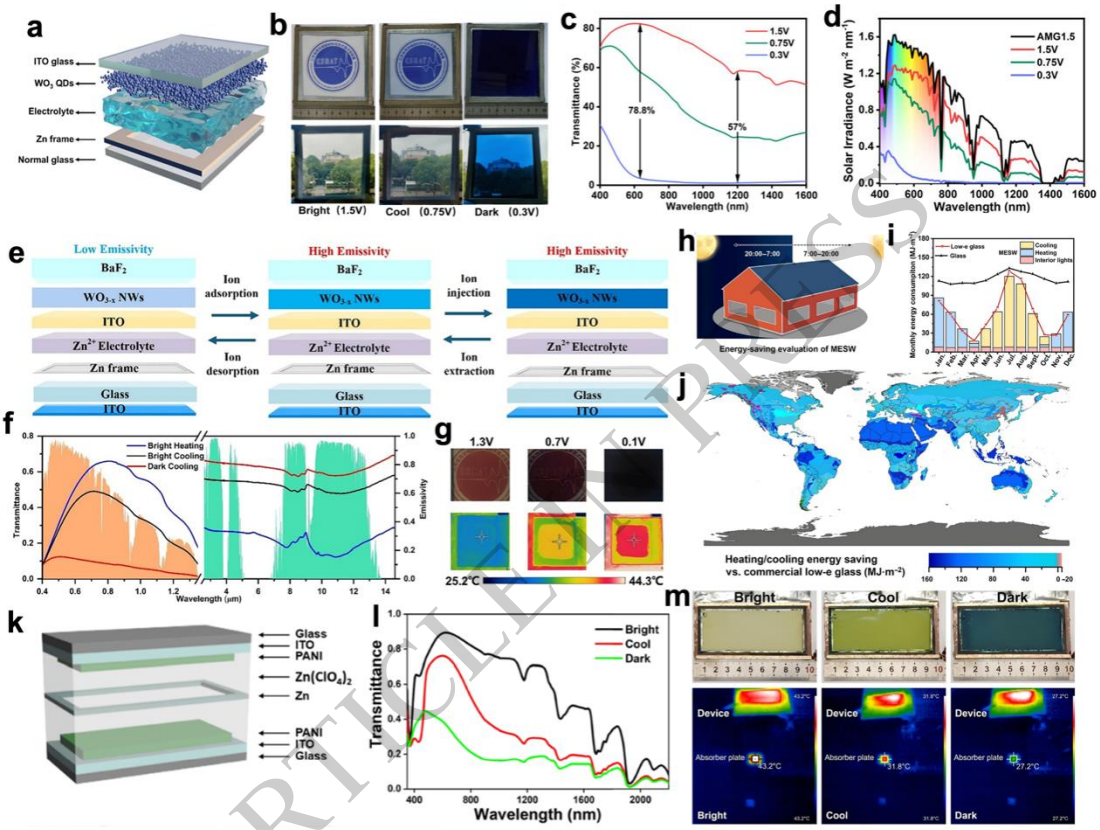


Figure 6. Electrochormic properties of ZDED[94]:(a) Schematic of the ZDED configuration. (b) Photographs of the ZDED (10 × 10 cm^2) operating in the bright, cool, and dark states, respectively. (c) Optical transmittance spectra and (d) solar irradiance spectra of the device. Copyright © 2026 Wiley-VCH GmbH. Performance of multicolor DESW devices[95]: (e) Schematic diagram of the device structure. (f) Transmission spectra of the fabricated devices in different modes; (g) Structure and operating principle of MESW. (h) Schematic of the prototypical small office building modeled in EnergyPlus. (i) Simulated monthly energy consumption of the MESW, low-e, and normal glass in Nanjing. (j) Global evaluation of heating/cooling energy savings: MESW versus commercial low-e glass across worldwide climate zones.

ARTICLE IN PRESS

Copyright © 2026 Tsinghua University Press and Springer-Verlag GmbH Germany, part of Springer Nature. PANI-based DESW device[96]: (k) Optical spectra of MESW in three modes. (l) Digital photographs and infrared images of MESW in three modes. (m) Photos of devices in ‘‘bright’’, ‘‘cool’’, and ‘‘dark’’ modes;Infrared thermal images of the absorber plate and device in the ‘‘bright’’, ‘‘cool’’, and ‘‘dark’’ modes under solar radiation for the same time. Copyright © 2023 The Royal Society of Chemistry.

Collectively, the aforementioned studies—spanning inorganic oxides and organic electrochromic materials—provide representative evidence supporting the feasibility [97, 98]. Furthermore, a subset of these devices integrates energy storage functionality-storing electrical energy during the coloring process and releasing it upon bleaching-thereby providing added value for self-powered building systems [99].

ARTICLE IN PRESS

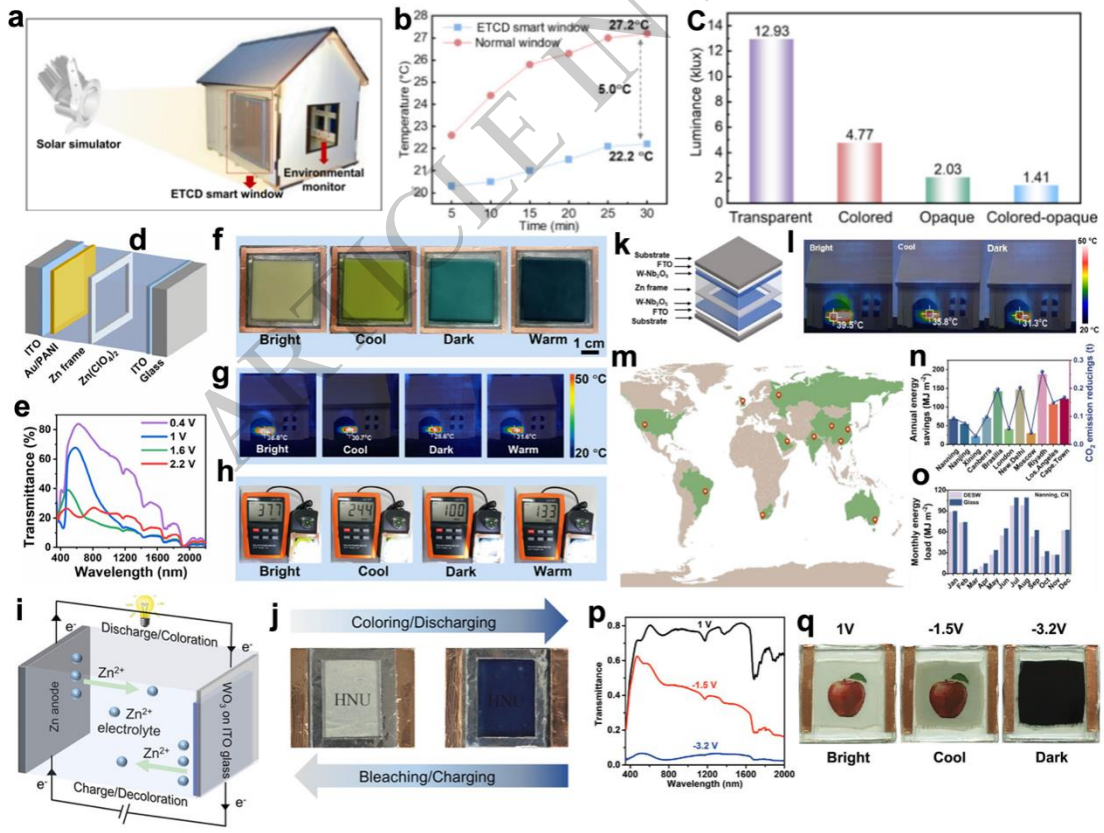


Figure 7. ETCD Smart Windows[100]: (a) Experimental setup for evaluating ETCD smart-window photothermal regulation. (b) Indoor temperature under solar

irradiation. (c) Indoor illuminance in four operating modes; Copyright © 2025 Elsevier B.V. Photothermal regulation of multicolor EC smart windows based on Au/PANI Schottky junctions[101]: (d) Schematic diagram of device structure. (e) Transmission spectra at different potentials. (f) Photos of the device in different modes. (g) Infrared thermal images of the device in four modes under simulated solar irradiation. (h) The luminous flux of the device under the same light source in four modes;Copyright © 2025 Wiley-VCH GmbH. Electrochromic and energy-storage performance of the Zn-WO_3 device[102]: (i) Schematic diagrams. (j) Digital photographs a Solar-charging performance of the 80 cm^2 ZECD smart window; Copyright © 2026 Wiley-VCH GmbH. Thermal regulation of DEWs and building energy efficiency simulation[41]: (k) Schematic of the device structure. (l) Infrared thermal image in “bright”, “cool”, and “dark” states under simultaneous AM 1.5 illumination. (m) Estimated heating and cooling energy saving of DEW in various cities representing different climate zones, relative to commercial glass. (n) Total annual energy savings for different cities across climate zones. (o) Monthly energy consumption of DEWs and conventional glass windows under Nanning climate conditions; Copyright © 2026 Wiley-VCH GmbH. Performance of the DBED[103]: (p) Optical transmittance spectra and (q) corresponding digital photos of the DBED in the bright (1 V), cool (-1.5 V), and dark (-3.2 V) modes, respectively; Copyright © 2020 Wiley-VCH GmbH.

ARTICLE IN PRESS

Sun et al.[100] designed a dual-responsive electrochromic-thermochromic (ETCD) smart window (**Figure 7**a), which combines a novel electrochromic film with a thermochromic electrolyte to achieve four operational states: bleached, colored, opaque, and colored-opaque. Miniature house model experiments demonstrated that the colored-opaque state reduced the indoor temperature by 5.0 °C compared to conventional windows (**Figure 7**b) and decreased indoor illuminance from 12.93 klux in the bleached state to 1.41 klux (**Figure 7**c), exhibiting superior synergistic optical and thermal management while simultaneously generating electrical energy during operation to power indoor lighting. Additionally, strategies utilizing Schottky

junctions to enhance electrochromic performance have also been employed to achieve multi-mode optical and thermal management. Cao et al. [101] constructed a multicolored electrochromic smart window (DESW) based on an Au/PANI Schottky junction film (**Figure 7**d), where the built-in electric field at the Au/polyaniline (PANI) interface facilitates electronic transitions among polarons, bipolarons, and quinoid structures, thereby enhancing the electrochemical performance of the film. The device exhibits four operational modes "bright" (0.4 V), "cool" (1 V), "dark" (1.6 V), and "warm" (2.2 V)-displaying pale yellow, green, blue, and blue-black colors, respectively (**Figure 7**e and **Figure 7**f). Under simulated solar irradiation, the absorber temperatures for the four modes were 38.8, 30.7, 28.6, and 31.6 °C, with corresponding luminous fluxes of 377, 244, 100, and 133 W m^{-2}, respectively; this achieved independent modulation of visible and near-infrared transmittance, validating the feasibility of multi-mode optical and thermal management (**Figure 7**g and **Figure 7**h). Regarding broad-temperature-window applications, Wan et al. [102] stabilized the electrode interface using a eutectic-polymer dual-network electrolyte; the fabricated Zn/WO_3 device maintained stable optical modulation performance over 1,000 cycles (**Figure 7**i), broadened the operating temperature range to -30 to 80 °C, and achieved reversible switching between transparent and blue states during charging (1.6 V) and discharging (0 V) (**Figure 7**j). Cao et al.[41] reported a dual-band electrochromic window (DEW) based on W-Nb_2O_5 films (**Figure 7**k). Under AM 1.5 G solar irradiation, the transmitted power densities for the "bright", "cold", and "dark" states of the DEW were 165, 29, and 6 W m^{-2}, maintaining the indoor fabric temperatures at 39.5 °C, 35.8 °C, and 31.3 °C, respectively (**Figure 7**l). EnergyPlus simulations showed that implementing these windows in Nanning and Riyadh achieved annual energy savings of 67.7 and 187.9MJ m^{-2} (corresponding to energy-saving efficiencies of 9.9% and 15.4%), reducing annual CO_2 emissions by 0.094 and 0.26 t m^{-2}, respectively (**Figure 7**m,n and **Figure 7**o). Zhang et al. [103] reported a single-component dual-band electrochromic device based on oxygen-deficient TiO_{2-x} nanocrystal films (**Figure 7**p,q). Operated within a potential range of 3.5-1.5 V (vs. Li^+/Li), the device exhibits outstanding optical modulation, achieving transmittance

ARTICLE IN PRESS

changes of 95.5% at 633 nm, 98.8% at 800 nm, 90.5% at 1200 nm, and 77.5% at 1600 nm. In the "cool" mode (1.8 V), it selectively blocks 77.1% of near-infrared (NIR) radiation while maintaining a high visible light transmittance of 66.0%. Upon switching to the "dark" mode (1.5 V), the rejection rates for visible light and NIR radiation reach 97.1% and 86.5%, respectively, demonstrating independent and highly efficient regulation across distinct spectral regions. These results demonstrate that electrochromic smart windows have exhibited promising practical prospects in optical and thermal management, broad-temperature-window stability, and energy self-sufficiency, providing experimental grounds for the multifunctional design of next-generation energy-efficient architectural glass.

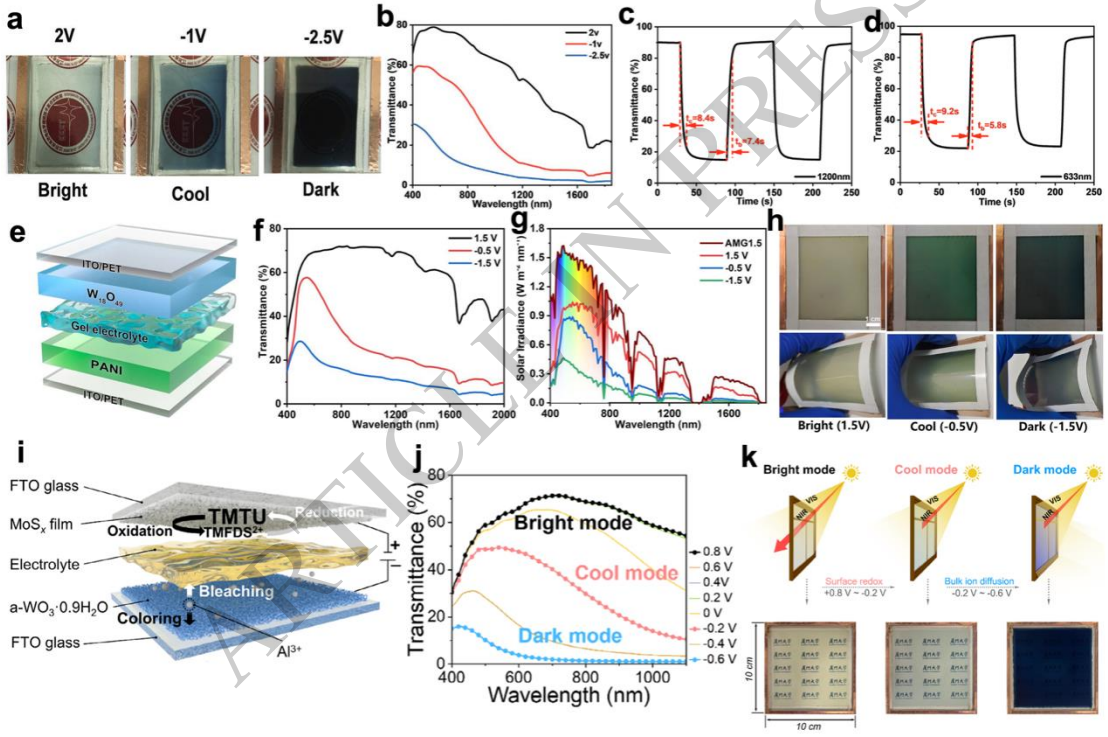


Figure 8. Electrochemical and electrochromic performance of AP-WO_3 films window[104]:(a) the corresponding digital photos of the DBED (active area 4×3 cm^2) in the bright, cool, and dark modes, respectively. (b) Optical transmittance spectra. Real-time transmittance spectra (c) at 1200 nm and (d) at 633 nm, respectively; Copyright © 2023 Wiley-VCH GmbH. Electrochormic properties of DBED[99]: (e)Schematic diagram of the flexible DBED based on a $W_{18}O_{49}$ NW cathode and a PANI anode. (f) Optical transmittance spectra, (g) solar irradiance spectra and (h) corresponding digital photos of DBED (size: 7 × 7 cm^2) in the bright (1.5 V), cool (− 0.5 V), dark (−

ARTICLE IN PRESS

1.5 V) modes; Copyright © 2025 Springer Nature. respectively Dual-Band Electrochromic Device Structure and Large-Area Demonstration[105]: (i) Schematical illustration of the architecture and working mechanism of a dual-band electrochromic device. (j) Optical transmittance spectra of the device held at indicated operational potentials for 60 s. (k) Schematic illustration and photographs of the large-area (10 cm × 10 cm) dual-band electrochromic smart window operating in bright, cool, and dark modes; Copyright © 2025 Wiley-VCH GmbH.

Zhang et al. [104] developed an amorphous porous WO_3 (AP-WO_3) film for fast single-component dual-band electrochromism without a sluggish phase transition. As a result, AP-WO_3 enables independent VIS/NIR regulation across three "bright-cool-dark" states (**Figure 8**a). The device achieved an optical modulation of 60.7% at 633 nm, while the cool state blocked 87.6% of NIR and maintained 53.9% VIS transmittance (**Figure 8**b). Fast switching was also demonstrated, with coloration/bleaching times of 8.4/7.4 s at 1200 nm and 9.2/5.8 s at 633 nm (**Figure 8**c,d). These results demonstrate the potential of AP-WO_3 for fast-switching single-component dual-band electrochromic smart windows. Building on this structural-regulation strategy, Zhang et al.[99] constructed a flexible full-cell dual-band electrochromic device (DBED) integrating a $W_{18}O_{49}$ nanowire cathode, a porous polyaniline (PANI) anode, and a gel electrolyte (**Figure 8**e). The porous PANI anode acts as both a charge-balancing layer and an optical enhancer, enabling a low operating voltage of 1.5 V. The device achieves independent VIS and NIR modulation across three distinct modes (Bright, Cool, and Dark; **Figure 8**f,g) with high optical contrast while maintaining robust switching performance under severe bending (**Figure 8**h), confirming its practical feasibility for scalable smart windows. While nanoscale structural engineering enhances ion transport and structural stability, manipulating the electrochemical reaction pathways offers another route toward selective dual-band regulation. Cheng et al.[105] demonstrated that structural-water engineering in amorphous WO_3 enables stepwise spectral regulation through surface redox and bulk Al^{3+} insertion, corresponding to NIR-selective and broadband

ARTICLE IN PRESS

VIS/NIR modulation, respectively (**Figure 8**i). The device exhibited transparent and dark states at +0.8 and −0.6 V, respectively, with VIS and NIR transmittances of 69.1% at 633 nm and 54.4% at 1100 nm in the transparent state; the lower transmittance than that of the WO_3 hydrate film was attributed to absorption by the counter electrode (**Figure 8**j). By tuning the applied potential, the device achieved distinct bright, cool, and dark states, while solution processing enabled a large-area device (100 cm^2) with clear optical-state switching (**Figure 8**k), demonstrating its potential for scalable dual-band electrochromic smart windows. Collectively, these studies underscore the importance of rationally regulating material structures and ion-electrode interactions in achieving independent, fast, and stable dual-band electrochromism.

Overall, single-component dual-band electrochromic materials provide the essential material foundation for transitioning electrochromic smart windows from single-band regulation to multi-band spectrally selective modulation. Future research must delve deeper into controllability in material synthesis, device interface stability, dual-band switching reliability, uniformity in large-area fabrication, and life-cycle energy consumption assessments under practical building environments.

ARTICLE IN PRESS

Table 2. Performance comparison between the electrochromic device developed in this work and previously reported electrochromic devices.

Materials	Voltage window	$\Delta T_{VIS}/\Delta T_{NIR}$	Response time (s)	Cycle stability	Active area (cm^2)	Electrolyte type	Coloration efficiency ($cm^2\ C^{-1}$)
WO_3-QD	0.3-1.5V	78.8%/57.0%	10.3/12.3	92.1% (10000 cycles)	/	Zn^{2+}/H^+	54.8

WO_{3-x}	0.1-1.3V	52.8%	2.6/4.6	99.78% (10000 cycles)	/	Zn^{2+}	101.9
PANI	0.4-1.7V	65/59%	1.0/1.9	94% (10000 cycles)	50	Zn^{2+}/PC	367.1/299.6
EC	0-0.8V	67.2%	36.8/15.8	86.7% (18000 cycles)	/	TC	286.5
Au/PANI	0.4-2.2V	54.6%	0.9/1.3 1.1/5.4	88.5% (200 cycles)	25	Zn^{2+}/PC	361.7
W-Nb2O3	-1.5-1.0V	92.3/93.8%	3.4/2.8 2.4/5.2	90% (100000 cycles)	/	Zn^{2+}	63.4/206.1
WO3	0-1.6V	58.3%	29.1/26.2	91% (1000 cycles)	/	Zn^{2+}	42
TiO_{2-x} NCs	1.5-3.5V	95.5/90.5%	35.1/9.6 15.5/3.4	95.6% (2000 cycles)	/	Li^{+}/PC	38.2/112.7
AP-WO_3	-2.5-2V	53.9/87.6%	9.2/5.8 8.4/7.4	75.5% (1000 cycles)	12	Li^{+}/PC	189.3 (1200nm)
$W_{18}O_{49}$NW	-1.5-1.5V	73.1/85.3%	8.8/15.6 5/11.2	96.7% (10000 cycles)	49	Li^{+}/PC	70.5/185

ARTICLE IN PRESS

To comprehensively evaluate and systematically compare the practical potential of the aforementioned dual-band electrochromic devices (DBEDs), Table 2 summarizes their benchmark performance metrics. Moreover, while most reported prototypes feature rapid switching dynamics and high cycling endurance, maintaining large active areas alongside robust optical contrast and operational durability remains a critical benchmark for future commercial scalability.

5.Challenges and Perspectives

Although electrochromic devices have made substantial progress in optical modulation, their practical applications remain constrained by the limited ability of conventional electrochromic materials to independently regulate visible (VIS) and near-infrared (NIR) light. Typically, strong coloration in the VIS region inevitably leads to a significant decrease in visible-light transmittance, compromising daylighting and limiting the flexibility of optical management in smart windows and wearable devices. Single-component dual-band electrochromic materials offer a promising strategy to overcome this limitation by decoupling VIS and NIR absorption, thereby enabling independent regulation of daylight and solar heat while maintaining high optical transparency when required. However, achieving such spectral selectivity requires precise control over redox potential distributions, ion diffusion kinetics, and electronic structures within a single material, together with rational structural engineering to simultaneously realize large optical modulation, fast switching, and long-term cycling stability. Furthermore, integrating these materials with flexible transparent substrates and intelligent control systems remains essential for translating dual-band electrochromic devices from laboratory demonstrations to practical applications.

From a long-term perspective, further development of single-component dual-band electrochromic technology should focus on several key aspects. First, quasi-solid-state and all-solid-state electrolytes with wide electrochemical windows, high ionic conductivity, and good interfacial compatibility should be developed to improve

ARTICLE IN PRESS

device safety, stability, and durability. while effectively mitigating continuous parasitic side reactions and contact degradation under repetitive volumetric changes to ensure long-term solid-electrolyte interfacial stability. Second, material and device architectures should be rationally engineered to achieve more precise and independent VIS/NIR modulation while minimizing optical and electrochemical interference between the two spectral bands. As well as resolving resistance-capacitance (RC) time constant delays and sheet-resistance-driven potential non-uniformities that currently hinder uniform large-area scaling. Third, scalable and low-cost synthesis and film-forming strategies, including solution-based deposition and environmentally benign processing, are highly desirable for large-area fabrication and practical manufacturing. which must also be coupled with rigorous life-cycle assessments (LCA) and cost-reduction strategies to guarantee sustainable commercial deployment. In this context, the recent emergence of advanced solution-processable n-type conducting polymers-such as poly(benzodifurandione) (PBFDO, or n-PBDF) systems offering electrical conductivity and ambient stability comparable to benchmark p-type PEDOT-represents a significant milestone, enabling robust, fast-switching, and scalable neutral-black devices[106, 107] . Finally, integration with adaptive control systems capable of responding to environmental parameters such as solar irradiance and temperature could enable autonomous switching among multiple optical states, providing dynamic management of daylighting, solar heat gain, and privacy. Furthermore, establishing universally standardized durability protocols for cross-laboratory benchmarking and clearly defining the operational separation between purely optical electrochromic systems (EC-only) and dual-function energy-storage devices will be essential. Collectively, these advances will be crucial for translating single-component dual-band electrochromism into scalable, intelligent, and energy-efficient smart-window technologies.

ARTICLE IN PRESS

6.Conclusion

Single-component dual-band electrochromic materials enable dynamic and selective regulation of visible (VIS) and near-infrared (NIR) transmittance within a single

electrochromic layer, offering a promising route toward multi-band optical management in smart windows. This review summarizes the major advances in this field from three perspectives: synthetic strategies, mechanistic understanding, and device applications. In inorganic systems, strategies including low-oxygen/reducing-atmosphere deposition, structural-water engineering, pre-intercalated ion regulation, wet-chemical doping, and morphology engineering enable decoupled VIS/NIR modulation through mechanisms such as oxygen-vacancy-induced localized surface plasmon resonance, potential separation mediated by structural water, sequential redox reactions of multiple valence states, and enhanced ion transport enabled by porous or helical architectures. In organic systems, molecular engineering and stepwise redox processes enable conducting polymers, small molecules, and metal complexes to exhibit distinct absorption bands at different potentials, thereby achieving dual-band optical modulation. At the device level, these materials enable reversible switching among multiple optical states, such as “bright-warm,” “bright-cool,” “dark-warm,” and “dark-cool,” providing flexible control over daylighting, solar-heat gain, and privacy. Despite these advances, challenges remain in intrinsic material stability, uniform and scalable fabrication, interfacial compatibility, and the lack of standardized performance evaluation, which collectively hinder the transition of single-component dual-band electrochromic devices from laboratory demonstrations to practical applications.

ARTICLE IN PRESS

Despite the impressive cycling stability demonstrated by numerous newly developed electrochromic materials in laboratory environments, the translation from academic research to commercial smart window products remains challenging. A critical missing link is the comprehensive evaluation of real-world device durability under harsh environmental conditions, such as prolonged high-temperature thermal stress, intense solar/UV irradiation, and moisture ingress. Unlike pristine material cyclic voltammetry tests, packaged commercial devices must withstand years of outdoor weathering without sealant failure, ion leakage, or optical degradation. Therefore, future efforts in the electrochromic community should pivot from merely pursuing

high optical modulation and basic cycling lifetimes toward developing robust encapsulation technologies, thermally stable electrolytes, and weather-resistant material configurations to truly bridge the gap between laboratory success and industrial deployment.

Declarations

Authors contribution

Lu Chen. Binbin Han and Chao Han contributed equally to this work.

Lu Chen, Binbin Liu, Chao Han: Writing-original draft, writing-review & editing.

Wei Wang, Mingxin Ma, Yuer He, Yiran Wang: Writing-review & editing.

Bing Ding, Shengliang Zhang and Xiaogang Zhang: Conceptualization, supervision

Declaration of Generative AI and AI-Assisted Technologies in the Writing Process

During the preparation of this manuscript, the author(s) used Gemini in order to polish language, improve grammatical accuracy, and refine the readability of the text. After using this tool/service, the author(s) reviewed and edited the content as needed and take(s) full responsibility for the content of the publication.

Conflicts of interest

The authors declare no conflicts of interest.

Ethical approval

Not applicable.

Consent to participate

Not applicable.

Consent for publication

Not applicable.

Availability of data and materials

ARTICLE IN PRESS

Not applicable.

Funding

This work was supported by the National Natural Science Foundation of China (62575137), Guangdong Basic and Applied Basic Research Foundation (2025A1515012067), China Postdoctoral Science Foundation (2022TQ0148, 2023M731651), Research Fund of State Key Laboratory of Mechanics and Control for Aerospace Structures (Nanjing University of Aeronautics and astronautics) (MCAS-I-0325G02), Shenzhen Longhua Science and Technology Innovation Special Funding Project (Industrial Sci-Tech Innovation Center of Low-Altitude Intelligent Networking. We also acknowledge the Center for Microscopy and Analysis at Nanjing University of Aeronautics and Astronautics.

Copyright

© The Author(s) 2026.

ARTICLE IN PRESS

References

1.Zhang C, Li S, Wu R, Wu S, Wang X, Xie H, et al. Robust MnO_2-WO_3 complementary electrochromic device enabled by reversible electrodeposition of MnO_2. Nano Lett. 2024;24(51):16360-16367. [DOI:10.1021/acs.nanolett.4c04849]

2.Zhang J, Tu JP, Xia XH, Qiao Y, Lu Y. An all-solid-state electrochromic device based on NiO/WO_3 complementary structure and solid hybrid polyelectrolyte. Sol Energy Mater Sol Cells. 2009;93(10):1840-1845. [DOI:10.1016/j.solmat.2009.06.025]

3.Chen J, Hu J, Wang B, Zhang H, Liang J, Shi P, et al. Solar and thermal dual-band electrochromic windows for energy-efficient buildings. Nat Commun. 2026;17:8882. [DOI:10.1038/s41467-026-75753-8]

4.Zhao F, Wang B, Huang B, Zhang W, Chen J, Liu L, et al. Inorganic electrochromic smart windows for advancing building energy efficiency. Nat Rev Clean Technol. 2025;1(6):396-412. [DOI:10.1038/s44359-025-00065-x]

5.Wang M, Lai W, Jiang W, Yang H, Chen L, Xu J, et al. Confined solid-state polyiodide deposition enables durable electrochromic smart windows. Adv Mater. 2026;38(56):e74530. [DOI:10.1002/adma.74530]

6.Wang C, Zhu L, Wang X, Tamer TM, Yao R, Rahman MM, et al. Application of nanocellulose in solar photo/thermal energy conversion and electrochemical energy storage devices. Green Carbon. 2025;3(3):225-245. [DOI:10.1016/j.greenca.2025.02.001]

7.Jessen W, Wilbert S, Gueymard CA, Polo J, Bian Z, Driesse A, et al. Proposal and evaluation of subordinate standard solar irradiance spectra for applications in solar energy systems. Solar Energy. 2018;168:30-43. [DOI:10.1016/j.solener.2018.03.043]

8.Wang D, Chen G, Fu J. Multifunctional thermochromic smart windows for building energy saving. J Mater Chem A. 2024;12(22):12960-12982. [DOI:10.1039/d4ta01767f]

9.Chen L, Guo X, Wang M, Jiang W, Cai S, Tang X, et al. Enhancing cycling stability of iodine electrodeposition electrochromic devices Assisted by liquid active adhesion material. Sol Energy Mater Sol Cells. 2026;297:114112. [DOI:10.1016/j.solmat.2025.114112]

10.Huang Y, Zhao Z, Wu X, Zhang R. Spectral engineering of electrochromic smart windows for energy-efficient buildings. Commun Mater. 2026;7:242. [DOI:10.1038/s43246-026-01361-0]

11.He D, Su C, Zhao C, Yan G, Zhao Z, Mai W. Multicolor electrochromic device based on reversible metal electrodeposition of Bi-Cu with controlled morphology and composition ratio. Chem Eng J. 2022;438:135469. [DOI:10.1016/j.cej.2022.135469]

12.Guo X, Chen J, Eh AL, Poh WC, Jiang F, Jiang F, et al. Heat-insulating black electrochromic device enabled by reversible nickel-copper electrodeposition. ACS Appl Mater Interfaces. 2022;14(17):20237-20246. [DOI:10.1021/acsami.2c02626 PMID:35467337]

13.Lou J, Zhu X, Li T, Yang X, Ma D, Zhu L, et al. Preparation and electrochromic properties of MnO_2/PPy composite films with coral-like structures. ACS Appl Mater Interfaces. 2024;16(28):36942-36952. [DOI:10.1021/acsami.4c05669]

ARTICLE IN PRESS

14.Xia Y, Zhou Y, Zhang B, Zhang Y, Zhang Y, Ma R. Recent progress and mechanisms of radiative thermal management smart windows: A review. Smart Mater Devices. 2026;2(2):202545. [DOI:10.70401/smd.2026.0026]

15.Cao S, Zhang S, Zhang T, Yao Q, Lee JY. A visible light-near-infrared dual-band smart window with internal energy storage. Joule. 2019;3(4):1152-1162. [DOI:10.1016/j.joule.2018.12.010]

16.Cao S, Zhang S, Zhang T, Lee JY. Fluoride-assisted synthesis of plasmonic colloidal Ta-doped TiO_2 nanocrystals for near-infrared and visible-light selective electrochromic modulation. Chem Mater. 2018;30(14):4838-4846. [DOI:10.1021/acs.chemmater.8b02196]

17.Barawi M, De Trizio L, Giannuzzi R, Veramonti G, Manna L, Manca M. Dual band electrochromic devices based on Nb-doped TiO_2 nanocrystalline electrodes. ACS Nano. 2017;11(4):3576-3584. [DOI:10.1021/acsnano.6b06664 PMID:28328197]

18.Meng Q, Cao S, Guo J, Wang Q, Wang K, Yang T, et al. Sol-gel-based porous Ti-doped tungsten oxide films for high-performance dual-band electrochromic smart windows. J Energy Chem. 2023;77:137-143. [DOI:10.1016/j.jechem.2022.10.047]

19.Guo X, Chen L, Liu R, Fan B, Cong S, Wang Z, et al. Ionic liquid $MPII_3$ elevates electrochromic battery capacity to practical applications. Adv Mater. 2025;37(29):e2504575. [DOI:10.1002/adma.202504575 PMID:40326178]

20.Guo X, Chen Y, Li S, Chen L, Xia S, Wang Q, et al. Color-neutral WO_3-I2 complementary electrochromic device based on reversible iodine electrodeposition. Chem Eng J. 2025;505:159726. [DOI:10.1016/j.cej.2025.159726]

21.Chen M, Deng J, Zhang H, Zhang X, Yan D, Yao G, et al. Advanced dual-band smart windows: Inorganic all-solid-state electrochromic devices for selective visible and near-infrared modulation. Adv Funct Mater. 2025;35(3):2413659. [DOI:10.1002/adfm.202413659]

22.Shao Z, Huang A, Cao C, Ji X, Hu W, Luo H, et al. Tri-band electrochromic smart window for energy savings in buildings. Nat Sustain. 2024;7(6):796-803. [DOI:10.1038/s41893-024-01349-z]

ARTICLE IN PRESS

23.Liang Y, Cao S, Guo J, Zeng R, Zhao J, Zou B. Dual-band electrochromic smart window based on single-component nanocrystals. ACS Appl Electron Mater. 2022;4(11):5109-5118. [DOI:10.1021/acsaelm.2c01225]

24.Du Z, Wang S, Gu C, Yang G. Recent advances in photo- or electro-chromic smart windows and their thermal regulation. Responsive Mater. 2025;3(2):e20250007. [DOI:10.1002/rpm.20250007]

25.Wan J, Chen Y, Li Z, Fan B, Guo X, Cong S, et al. Electrochromism enabled by Br^-/Br_3^- conversion. Nano Lett. 2025;25(28):11134-11141. [DOI:10.1021/acs.nanolett.5c02633]

26.Li S, Chen Y, Wang Z, Wang M, Guo X, Tang X, et al. Electrochromism via reversible electrodeposition of solid iodine. Nat Commun. 2025;16:724. [DOI:10.1038/s41467-024-55348-x]

27.Liao L, Fu X, Cao Z, Chen W, Rogachev AA, Yarmolenko MA, et al. Quasi-solid-state electrochromic energy storage devices with long-term stability. ACS Appl Polym Mater. 2025;7(10):5910-5919. [DOI:10.1021/acsapm.5c00172]

28.Zhou J, Huang Z, Han C, Qi P, Wang J, Zhang S. Research progress on single-component dual-band electrochromic materials and devices. China Tungsten Ind. 2025;40(3):13-23. Available from: https://link.cnki.net/urlid/11.3236.TF.20250516.1429.002

29.Hassan M, Ghaffar A, Lou G, Miao Z, Peng Z, Celebi K. Enhanced transport kinetics of electrochromic devices by $W_{18}O_{49}$ NW/$Ti_3C_2t_x$ composite films. Adv Funct Mater. 2024;34(27):2310535. [DOI:10.1002/adfm.202310535]

30.Zhou D, Deng Q, Yang L. Stable and high-performance polyaniline/V_2CT_x MXene composite electrochromic films prepared by one-pot electrodeposition method. Polymers. 2025;17(22):3079. [DOI:10.3390/polym17223079 PMID:41304442 PMCID:PMC12656005]

31.Zhang Q, Ju S, Zhang S, Xu S, Zhang Z. A multi-colored, structure-tolerant vanadate cathode for high-performance aqueous zinc-ion batteries. Adv Energy Mater. 2025;15(18):2404597. [DOI:10.1002/aenm.202404597]

32.Wu C, Zhang Y, Shi H, Yu J, Yang Y, Zhang C, et al. High-performance

ARTICLE IN PRESS

complementary electrochromic batteries using $Nb_{18}W_{16}O_{93}$ by the synergistic effects of aqueous Al^{3+}/K^{+} dual-ion. Angew Chem. 2025;137(3):e202415050. [DOI:10.1002/ange.202415050]

33.Chen T, Xu B, Zhou G, Wu W, Huang B, Tang X, et al. Advancing energy efficiency in smart windows via dual-responsive electro-thermochromism. Adv Sci. 2026;13(60):e77055. [DOI:10.1002/advs.77055]

34.Cai G, Cui M, Kumar V, Darmawan P, Wang J, Wang X, et al. Ultra-large optical modulation of electrochromic porous WO_3 film and the local monitoring of redox activity. Chem Sci. 2016;7(2):1373-1382. [DOI:10.1039/c5sc03727a PMID:29910894 PMCID:PMC5975915]

35.Wang C, Xiang S, Chen L, Liang L, Tu J, Shen S, et al. In situ formation of LiF-rich SEI in quasi-solid electrolytes enables long-life electrochromic devices. Adv Mater. 2026;38(7):e16702. [DOI:10.1002/adma.202516702 PMID:41261818]

36.Thiyagarajan D, Thirumurugan A, Lin J, Lee BK. Performance optimization and functional integration in emerging electrochromic device architectures. J Phys: Condens Matter. 2026;38(25):253004. [DOI:10.1088/1361-648x/ae76a5]

37.Huang Y, Wu S, Zhao S, Guo Z, Zhao Z, Wu X, et al. A novel liquid flow electrochromic smart window for all-year-round dynamic photothermal regulation. Energy Environ Sci. 2025;18(4):1824-1834. [DOI:10.1039/d4ee05416d]

38.Wang J, Weng J, Wang L, Zhou Y, Chen H, Xie A, et al. Amorphous hydrated tungsten oxide films with electrochromic cycling stability up to 40 000 cycles enabled by regulating the coloring potential and structural water. ACS Appl Mater Interfaces. 2025;17(45):62285-62296. [DOI:10.1021/acsami.5c14394 PMID:41152010]

39.Sun X, Wang D, Wu W, Zhao X, Zhang X, Wang B, et al. Amorphous and crystalline Ti-doped $WO_3 \cdot 2H_2O$ for dual-band electrochromic smart windows. ACS Sustainable Chem Eng. 2024;12(14):5459-5467. [DOI:10.1021/acssuschemeng.3c07679]

40.Huo X, Shen J, Wang Z, Zhang M, Guo M. Bistable visible-near-infrared dual-band electrochromic materials with dynamical light/heat modulation performance based on the synergetic effect between TiO_2/WO_3 composite nanorod arrays and

ARTICLE IN PRESS

aqueous Al^{3+}. Adv Opt Mater. 2026;14(18):e71231. [DOI:10.1002/adom.71231]
41.Liu Y, Cao S, Su Y, Bao L, Liang R, Liang Y, et al. Ultra-stable dual-band electrochromic windows enabled by shear-phase niobium oxide. Adv Energy Mater. 2026;16(11):e05972. [DOI:10.1002/aenm.202505972]
42.Jia H, Ji X, Shao Z, Li Z, Huang A, Wen Z, et al. Li^{+}/Al^{3+} composite solid electrolyte based electro-thermal dual responsive devices with optimized optical contrast and cycle durability. Adv Opt Mater. 2022;10(11):2200106. [DOI:10.1002/adom.202200106]
43.Ma D, Yang T, Feng X, Wang P, Huang J, Wang J, et al. Quadruple control electrochromic devices utilizing $Ce_4W_9O_{33}$ electrodes for visible and near-infrared transmission intelligent modulation. Adv Sci. 2024;11(14):e2307223. [DOI:10.1002/advs.202307223 PMID:38311586 PMCID:PMC11005709]
44.Chen M, Zhang X, Yan D, Deng J, Sun W, Li Z, et al. Oxygen vacancy modulated amorphous tungsten oxide films for fast-switching and ultra-stable dual-band electrochromic energy storage smart windows. Mater Horiz. 2023;10(6):2191-2203. [DOI:10.1039/d2mh01472f PMID:36994625]
45.Li P, Lv Y, You X, Ma H, Wang T, Shen Y, et al. Bio-inspired ordered WO_3 nano-helixes enable multi-band electrochromic smart windows with ultrafast switching and robust cyclability. Energy Environ Mater. 2026;9(3):e70185. [DOI:10.1002/eem2.70185]
46.Zhang C, Chen Y, Wang X, Wang J, Chen J, Xie H, et al. High-capacity electrochromic battery enabled by inverted fabry–Pérot nanocavity. ACS Photonics. 2025;12(12):6671-6679. [DOI:10.1021/acsphotonics.5c01715]
47.Shi Y, Sun M, Zhang Y, Cui J, Shu X, Wang Y, et al. Rational design of oxygen deficiency-controlled tungsten oxide electrochromic films with an exceptional memory effect. ACS Appl Mater Interfaces. 2020;12(29):32658-32665. [DOI:10.1021/acsami.0c06786 PMID:32610893]
48.Li K, Yin Y, Diao P. Enhancing photoelectrochemical water oxidation on WO_3 via electrochromic modulation: Universal effects and mechanistic insights. Small. 2024;20(40):e2402474. [DOI:10.1002/smll.202402474 PMID:38822710]

ARTICLE IN PRESS

49.Guillén C, Herrero J. Amorphous WO_3- thin films with color characteristics tuned by the oxygen vacancies created during reactive DC sputtering. J Mater Sci Technol. 2021;78:223-228. [DOI:10.1016/j.jmst.2020.11.036]
50.Yang J, Wang M, Djeffal A, Wang S, Meng Z, Xu X, et al. Selective infrared thermal modulation device based on mixed-crystalline WO_3 and electrochromic dynamic regulation technology. Chem Eng J. 2026;544:179297. [DOI:10.1016/j.cej.2026.179297]
51.Huang Y, Wang B, Lyu P, Zhao S, Wu X, Zhang S, et al. Oxygen-deficient tungsten oxide nanoflowers for dynamically tunable near-infrared light transmittance of smart windows. Nano Res. 2023;16(10):12165-12172. [DOI:10.1007/s12274-023-5600-7]
52.Zhang R, Yin M, Shao P, Huang Q, Niklasson GA, Wen RT. Polaron hopping induced dual-band absorption in all amorphous cathodic electrochromic oxides. Appl Phys Rev. 2025;12(1):011404. [DOI:10.1063/5.0244549]
53.Li H, McRae L, Firby CJ, Elezzabi AY. Rechargeable aqueous electrochromic batteries utilizing Ti-substituted tungsten molybdenum oxide based Zn^{2+} ion intercalation cathodes. Adv Mater. 2019;31(15):e1807065. [DOI:10.1002/adma.201807065 PMID:30803069]
54.Zhao F, Li C, Li S, Wang B, Huang B, Hu K, et al. Continuous solar energy conversion windows integrating zinc anode-based electrochromic device and IoT system. Adv Mater. 2024;36(35):2405035. [DOI:10.1002/adma.202405035]
55.Mobtakeri S, Habashyani S, Budak HF, Gür E. Simultaneous amperometric and gasochromic measurements of α-MoO_3 gas sensors optimized with controlled content of Pd sensitizer and device configuration. Appl Surf Sci. 2025;704:163446. [DOI:10.1016/j.apsusc.2025.163446]
56.Zhai Y, Li J, Shen S, Zhu Z, Mao S, Xiao X, et al. Recent advances on dual-band electrochromic materials and devices. Adv Funct Mater. 2022;32(17):2109848. [DOI:10.1002/adfm.202109848]
57.Huang H, Li Y, Mo X, Li S, Cai G, Hu B. Lattice engineering of niobium tungsten titanium oxide metamaterial paired with multi-ionic electrolyte for high performance electrochromic devices. Adv Funct Mater. 2026;36(75):e77688.

ARTICLE IN PRESS

[DOI:10.1002/adfm.77688]
58.Zhang L, Wu J, Pan C, Zeng H, Li Y, Gao Y. Layer-stacked polyaniline/silver nanowire composite film for multicolor electrochromic smart windows with dual-band optical modulation. Opt Mater. 2024;150:115281. [DOI:10.1016/j.optmat.2024.115281]
59.Wu N, Ma L, Zhao S, Xiao D. Novel triazine-centered viologen analogues for dual-band electrochromic devices. Sol Energy Mater Sol Cells. 2019;195:114-121. [DOI:10.1016/j.solmat.2019.03.005]
60.Feng K, Li Z, Liu Y, Pei X, Wu Y, Zhou F. Self-assembled iridescent electrochromic platform with tunable infrared emissivity for adaptive visible-infrared dual-band camouflage in dynamic environments. ACS Appl Mater Interfaces. 2026;18(7):12188-12198. [DOI:10.1021/acsami.5c24670 PMID:41672925]
61.Raj MRA, Humeniuk HV, Skene WG. Covalent attachment strategies of molecular electrochromes for enhancing electrochromic performance. Chempluschem. 2025;90(9):e202500178. [DOI:10.1002/cplu.202500178 PMID:40765274 PMCID:PMC12435114]
62.Gao D, Zhao S, Huang Y, Wu X, Li R, Ding Y, et al. A facile electrochemical strategy for achieving a high-conductivity polypyrrole derivative with intrinsic metallic transport as a high-performance electrochromic conducting polymer film. Nano Lett. 2024;24(46):14854-14861. [DOI:10.1021/acs.nanolett.4c04570 PMID:39499111]
63.Zhu M, Wang W, He T, Xu B, Niu C, Zhou G, et al. Dynamic information transmission and encryption by stacked electrochromic device. Adv Funct Mater. 2026;36(54):e76530. [DOI:10.1002/adfm.76530]
64.Wu Z, Zhao Q, Luo X, Ma H, Zheng W, Yu J, et al. Low-cost fabrication of high-performance fluorinated polythiophene-based vis-NIR electrochromic devices toward deformable display and camouflage. Chem Mater. 2022;34(22):9923-9933. [DOI:10.1021/acs.chemmater.2c01964]
65.Wu X, Fan Q, Bai Z, Zhang Q, Jiang W, Li Y, et al. Synergistic Interaction of Dual-Polymer Networks Containing Viologens-Anchored Poly(ionic liquid)s

ARTICLE IN PRESS

Enabling Long-Life and Large-Area Electrochromic Organogels. Small. 2023;19(37):2301742. [DOI:10.1002/smll.202301742]

66.Zhang Y, Liang L, Gong C, Zhu L, Dong R, Fang J, et al. Interlayer UV-photo-cross-linking endowed PEDOT: PSS-based electrochromic smart windows with highly conductive and physically/chemically multicross-linked mechanical architectures. ACS Appl Mater Interfaces. 2025;17(49):66965-66979. [DOI:10.1021/acsami.5c20164 PMID:41314693]

67.Cao N, Lang Y, Gu G, Jia X, Chao D. Mixed ionic-electronic conducting polymer enables efficient electrochromic supercapacitor. Adv Funct Mater. 2026;36(13):e17668. [DOI:10.1002/adfm.202517668]

68.Du C, Cheng X, Zhang G, Xu J, Zhang J, Nie G, et al. Molecular bonding engineering enables ultra-stable electrochromic energy storage in flexible PEDOT devices. Adv Mater. 2026;38(8):e16740. [DOI:10.1002/adma.202516740]

69.Bhattacharjee S, Paul S, Puthiyaparambath MF, Thapa R, Kundu S. Orientation-selective and vacancy-engineered PANI-V_2O_5 nanocomposites for ultrafast high contrast quadri colored electrochromism. Mater Today Nano. 2026;35:100865. [DOI:10.1016/j.mtnano.2026.100865]

70.Liu D, Li N, Fan Q, Liu W, Zhang Y, Xu L, et al. Reversible metal electrodeposition assisting polyaniline for tri-mode adaptive radiative thermoregulation devices. Chem Eng J. 2025;526:170665. [DOI:10.1016/j.cej.2025.170665]

71.Wang Y, Zhang L, Xu L, Zhang Y, Yang R, Lv Z, et al. Acid-treated carbon nanotubes form a dual-continuous “electron-ion” transport network to enhance the remarkable dynamic thermal regulation properties of polyaniline. J Mater Chem A. 2026;14(51):35228-35239. [DOI:10.1039/d6ta03942a]

72.Zhai M, Ma C, Ma D, Huang X, Cai W, Zhou T, et al. Unlocking the secrets of color: Molecular engineering of triphenylamine-π-phenanthrimidazole polyamides for transparent-to-kaleidoscopic/black electrochromic switching. Chem Eng J. 2026;544:179240. [DOI:10.1016/j.cej.2026.179240]

73.Zhu C, Hou J, Wang X, Wang S, Xu H, Hu J, et al. Optimizing ligand-to-metal

ARTICLE IN PRESS

charge transfer in metal–organic frameworks to enhance photocatalytic performance. Chem Eng J. 2024;499:156527. [DOI:10.1016/j.cej.2024.156527]
74.Check B, Choi JY, Santarelli J, Lu C, Pham HTB, Lopez G, et al. Harnessing truxone-based electrically conductive metal-organic framework for electrochromism. J Am Chem Soc. 2025;147(51):46806-46811. [DOI:10.1021/jacs.5c17399 PMID:41389191]
75.Shi W, Zhou J, Xiong Y, Chen W. Regulating electron transfer through imine linkage orientations in two-dimensional covalent organic frameworks for efficient electrochromism. Chem Eng J. 2025;516:164278. [DOI:10.1016/j.cej.2025.164278]
76.Zhang W, Ding Y, Liu X, Ai D, Zhang Y, Zhang R, et al. In situ ion exchange mediated by carbon dots enables the preparation of multicolor Prussian blue analogues for high-performance electrochromic devices. Chem Eng J. 2026;532:174214. [DOI:10.1016/j.cej.2026.174214]
77.Feng K, Xing Z, Shi X, Tian J, Zhang H, Wu ZQ, et al. Electrochemically crosslinked poly(arylene ether sulfone)-triphenylamine electrochromic polymer networks for smart windows. Chem Eng J. 2026;548:181494. [DOI:10.1016/j.cej.2026.181494]
78.Qin L, Liu Y, Long M, Zou B, Cao S. Advancements in dual-band electrochromic smart windows: Exploring single-component materials for sustainable building solutions. Ceram Int. 2024;50(13):22174-22183. [DOI:10.1016/j.ceramint.2024.03.380]
79.Sun H, Wang W, Pan S, Jian Z, Xiong Y, Chen W. High-performance dual-band electrochromic materials based on Prussian white. J Alloys Compd. 2024;981:173732. [DOI:10.1016/j.jallcom.2024.173732]
80.Ji Y, Xu Q, Liu S, Xu B, Chen J. Smart electrochromic devices based on reversible (non-) metal electrodeposition. Smart Mater Devices. 2026;2(4):202637. [DOI:10.70401/smd.2026.0043]
81.Wang J, Guo X, Bian C, Zhong Y, Tu J, Lee PS, et al. Roadmap for electrochromic smart devices: From materials engineering and architectures design to multifunctional application. Prog Mater Sci. 2025;153:101461. [DOI:10.1016/j.pmatsci.2025.101461]

ARTICLE IN PRESS

82.Bi H, Wang X, Xu L, Zhao H, Fan L, Xuan J, et al. Structure-dependent trap passivation in WO_3 enables ultra-stable electrochromic devices. Adv Funct Mater. 2026;36(52):e76298. [DOI:10.1002/adfm.76298]

83.Zhao H, Yu X, Yu S, Yang H, Guo W, Li S, et al. Review on amorphous WO_3 for electrochromic devices: Structure, optimization strategies and applications. Mater Today Chem. 2025;43:102513. [DOI:10.1016/j.mtchem.2025.102513]

84.Minh NH, Kim K, Kang DH, Yoo YE, Yoon JS. Mechanically tunable mechanochromic device with covert-overt structural color and modulation of its transparency. Adv Mater Int. 2026;13(4):e00640. [DOI:10.1002/admi.202500640]

85.Wang Y, Sun X, Liu Q, Yu G. Functional gel materials for next-generation electrochromic devices and applications. Chem Soc Rev. 2025;54(7):3475-3512. [DOI:10.1039/d4cs01256a PMID:40019199]

86.Wang JL, Sheng SZ, He Z, Wang R, Pan Z, Zhao HY, et al. Self-powered flexible electrochromic smart window. Nano Lett. 2021;21(23):9976-9982. [DOI:10.1021/acs.nanolett.1c03438]

87.Zheng T, Zhang H, Chen C, Tu X, Fang L, Zhang M, et al. Self-powered dual-band electrochromic supercapacitor devices for smart window based on ternary dielectric triboelectric nanogenerator. Nanomaterials. 2024;14(2):229. [DOI:10.3390/nano14020229]

88.Wu W, Tian M, Tang Y, Song C, Zheng R, Guo Y, et al. Revolutionizing dual-band modulation and superior cycling stability in GDQDs-doped WO_3 electrochromic films for advanced smart window applications. Small. 2025;21(6):e2407708. [DOI:10.1002/smll.202407708 PMID:39780529]

89.Li R, Lan F, Tang L, Huang Y, Zhao S, Wang B, et al. A local-dissociation solid-state polymer electrolyte with enhanced Li^+ transport for high-performance dual-band electrochromic smart windows. Adv Funct Mater. 2025;35(15):2419357. [DOI:10.1002/adfm.202419357]

90.Bai T, Li W, Fu G, Zhang Q, Zhou K, Wang H. Dual-band electrochromic smart windows towards building energy conservation. Sol Energy Mater Sol Cells. 2023;256:112320. [DOI:10.1016/j.solmat.2023.112320]

ARTICLE IN PRESS

91.Liu R, Li Y, Hu B, Long Y. Organic ligand-free scalable dual-band electrochromic smart windows. Adv Funct Mater. 2024;35(1):2409914.
[DOI:10.1002/adfm.202409914]
92.Sui C, Pu J, Chen TH, Liang J, Lai YT, Rao Y, et al. Dynamic electrochromism for all-season radiative thermoregulation. Nat Sustain. 2023;6(4):428-437.
[DOI:10.1038/s41893-022-01023-2]
93.Zhang X, Hao L, Xie J, Tan Z, Li S, Gan C, et al. Multifunctional integrated electrochromic device by p-n conductive polymers for self-powered smart windows and miniaturized spectrometers. Nat Commun. 2025;16(1):11574.
[DOI:10.1038/s41467-025-67903-1]
94.Huang Z, Wang J, Zhang S, Wu L, Wu H, Xia X, et al. High-performance zinc-anode dual-band electrochromic devices based on tungsten oxide quantum dots for all-season building energy savings. Adv Funct Mater. 2026;36(39):e74565.
[DOI:10.1002/adfm.74565]
95.Qi P, Zhang S, Yuan L, Chen P, Han C, Huang Z, et al. All-season multiband electrochromic smart windows for dynamically compatible regulation of solar and thermal radiation. Nano Res. 2026;19(11):94908595.
[DOI:10.26599/NR.2026.94908595]
96.Wang Q, Cao S, Meng Q, Wang K, Yang T, Zhao J, et al. Robust and stable dual-band electrochromic smart window with multicolor tunability. Mater Horiz. 2023;10(3):960-966. [DOI:10.1039/d2mh01365g PMID:36606592]
97.Zhang W, Wang Z, Liu Z, Zhang L, Ma H, Fu J, et al. Enhanced electrochromic performance of Al-doped NiO films via magnetron sputtering: Experimental characterization and first-principles insights. Chem Eng J. 2026;546:180054.
[DOI:10.1016/j.cej.2026.180054]
98.Zhu Y, Li Y, Li J, Hong X, Jiang W, Zhu L. Power-free spontaneous galvanic deposition of high-purity Prussian blue films for multicolored textile electrochromic devices. Chem Eng J. 2026;547:180341. [DOI:10.1016/j.cej.2026.180341]
99.Huang Z, Peng Y, Zhao J, Zhang S, Qi P, Qu X, et al. An efficient and flexible bifunctional dual-band electrochromic device integrating with energy storage.

ARTICLE IN PRESS

Nanomicro Lett. 2024;17(1):98. [DOI:10.1007/s40820-024-01604-0 PMID:39729147 PMCID:PMC11680540]

100.Sun F, Wu H, Li M, Xu Y, Yan Y, Chen Y, et al. Smart window with high solar blocking capability: Integrating electrochromic TiO_2-viologen composite film and thermochromic electrolyte. Chem Eng J. 2025;521:166975. [DOI:10.1016/j.cej.2025.166975]

101.Huang L, Cao S, Liu Y, Chen J, Li H, Liang Y, et al. Built-In electric field-assisted polyaniline for boosting dual-band electrochromic smart windows with multicolor displays and four-mode conversion. Adv Funct Mater. 2025;35(37):2500064. [DOI:10.1002/adfm.202500064]

102.Wan J, Tan X, Li C, Leng M, Chen X, Pan A. Manipulating interfacial water molecules via eutectic-polymer dual-network for stable electrochromic devices. Angew Chem Int Ed Engl. 2026;65(37):e1941770. [DOI:10.1002/anie.1941770 PMID:42423231 PMCID:PMC13549028]

103.Zhang S, Cao S, Zhang T, Lee JY. Plasmonic oxygen-deficient TiO_{2-x} nanocrystals for dual-band electrochromic smart windows with efficient energy recycling. Adv Mater. 2020;32(43):e2004686. [DOI:10.1002/adma.202004686 PMID:32954545]

104.Zhang S, Peng Y, Zhao J, Fan Z, Ding B, Lee JY, et al. Amorphous and porous tungsten oxide films for fast-switching dual-band electrochromic smart windows. Adv Opt Mater. 2023;11(1):2202115. [DOI:10.1002/adom.202202115]

105.Zhang Z, Zhuang D, Niu Y, Wang J, Zhang H, Cheng W. High-performance dual-band electrochromic smart windows based on amorphous tungsten oxide hydrate films and aluminum ion electrolytes. Adv Opt Mater. 2025;13(12):2402526. [DOI:10.1002/adom.202402526]

106.Jin W, Jin T, Hu Z, Tang H, Huang F. Black electrochromic devices based on a highly conductive n-type polymer and a bilayer structure. J Mater Chem C. 2026;14(30):13600-13606. [DOI:10.1039/d6tc01224h]

107.Lee WJ, Mehra P, Thurston JR, Tian Y, Liu X, Samal S, et al. Robust fast-switching black electrochromic windows based on solution-processed n-doped

ARTICLE IN PRESS

transparent organic conductor. Nat Commun. 2025;17:575. [DOI:10.1038/s41467-025-67271-w]

ARTICLE IN PRESS